

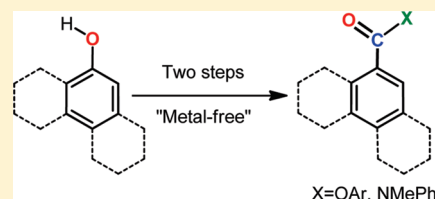
Radical O→C Transposition: A Metal-Free Process for Conversion of Phenols into Benzoates and Benzamides

Abdulkader Baroudi, Jeremiah Alicea, Phillip Flack, Jason Kirincich, and Igor V. Alabugin*

Department of Chemistry and Biochemistry, Florida State University, Tallahassee, Florida 32306, United States

Supporting Information

ABSTRACT: We report a metal-free procedure for transformation of phenols into esters and amides of benzoic acids via a new radical cascade. Diaryl thiocarbonates and thiocarbamates, available in a single high-yielding step from phenols, selectively add silyl radicals at the sulfur atom of the C=S moiety. This addition step, analogous to the first step of the Barton–McCombie reaction, produces a carbon radical which undergoes 1,2 O→C transposition through an *O*-neophyl rearrangement. The usually unfavorable equilibrium in the reversible rearrangement step is shifted forward via a highly exothermic C–S bond scission in the *O*-centered radical, which furnishes the final benzoic ester or benzamide product. The metal-free preparation of benzoic acid derivatives from phenols provides a potentially useful alternative to metal-catalyzed carbonylation of aryl triflates.



INTRODUCTION

Direct connections between functional groups simplify chemical landscape and allow more efficient execution of multistep synthetic routes. While phenols and benzoic acid derivatives are among the most common organic functionalities, the ways for transforming a phenol into an aryl carboxylic acid derivative are still limited. A metal-free reaction which converts phenols into benzoic acid derivatives would become a useful alternative to the commonly used Pd-catalyzed carbonylation of aromatic triflates¹ (Figure 1), especially because Pd is classified as a Class I metal (significant safety concern) in pharmaceuticals with permitted daily exposure <10 μg/day.² Herein, we report the design of an efficient metal-free O→C transposition, accomplished via a new radical cascade transformation of diaryl thiocarbonates and thiocarbamates into carboxylic esters and amides. In this process, the classic Barton–McCombie reaction is diverted into the *O*-neophyl pathway driven by a strategically introduced radical fragmentation.

The key components of our proposed synthetic design came from our work on unraveling the mechanism of esperamycin A₁ fragmentation,³ which follows Bergman cyclization⁴ of this natural enediyne antibiotic. When we equipped model enediynes with acetal rings mimicking the carbohydrate moiety of the natural enediyne antibiotics, we found that several interesting radical rearrangements triggered by the Bergman cyclization (Figure 2) including the O→C transposition of enediyne **2** (Figure 2b).⁵ Although the yield for the rearranged benzoic ester **3** was low, this result suggested that this process, which could serve as a synthetic shortcut between phenols and benzoates, is possible, prompting us to search for a more efficient version of this transformation.

Several factors are important for a successful design of the more efficient O→C transposition (Figure 3). First, phenols should be converted readily to a functional precursor of a phenoxy-substituted carbon radical. Second, this radical should initiate the key transposition step which we envisioned to proceed

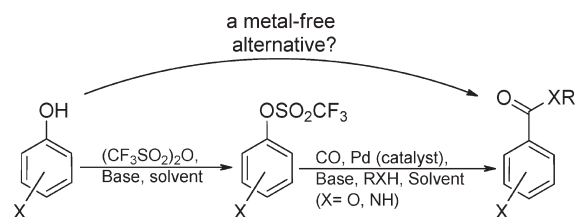


Figure 1. Metal-catalyzed transformation of phenols into benzoic acid derivatives.

through an *O*-neophyl rearrangement.^{6,7} Consequently, substituents X and Z should neither deactivate the carbon radical center nor participate in a premature β-scission step (Figure 3). Finally, since the *O*-neophyl rearrangement is reversible, a fast and selective fragmentation route via efficient β-scission of a weak C–X bond should be available in order to trap the transposed radical. This fragmentation should not only complete the rearrangement via formation of the C=O double bond in the final product but also generate a new S-centered radical for propagating the radical chain process.⁸

The crucial role of the final fragmentation step in driving the rearrangement from a more stable C-radical to a less stable *O*-radical is illustrated by the fact that most literature examples of radical *O*-neophyl rearrangements proceed in the opposite direction, from alkoxy radicals to the more stable carbon radicals.^{9,10} To the best of our knowledge, before our preliminary disclosure of this work,¹¹ there was only one example where the reaction followed the same rearrangement pathway as enediyne **2**. Ohno et al. reported the formation of methylphenylketone in about 50% yield from the thermal decomposition of azobis-(2-phenoxy)-2-propane (Figure 4).¹² Interestingly, in analogy

Received: December 31, 2010

Published: February 23, 2011

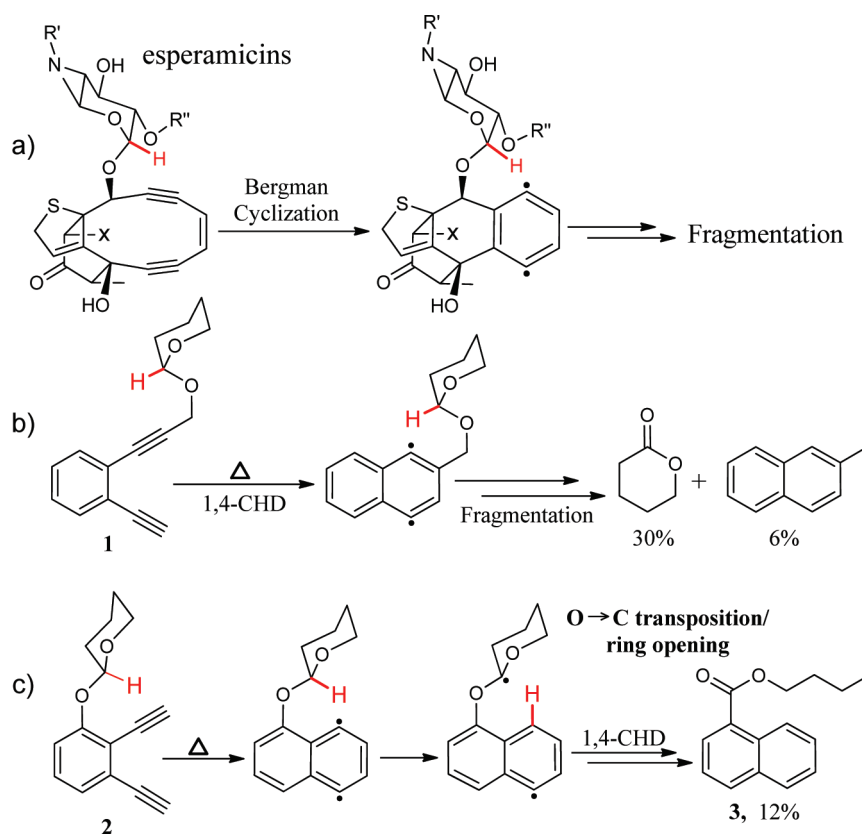


Figure 2. (a) Fragmentation of natural enediyne. (b) Fragmentation of esperamicine mimics through intramolecular H-abstraction/fragmentation cascade. (c) O→C radical transposition triggered by the Bergman cyclization of enediyne 2.

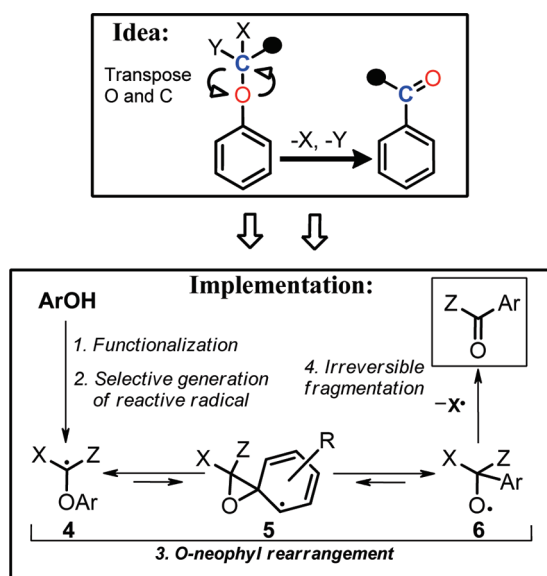


Figure 3. Suggested design of an efficient radical 1,2 O→C transposition cascade.

with the reaction observed for **2**, these authors found that the O-neophyl rearrangement of 2-phenoxyprop-2-yl radical into 2-phenylisopropoxy radical is also terminated by a homolytic C–C bond cleavage. In our case, the bond cleavage leads to the ring-opening of the THP moiety, whereas for the formation of

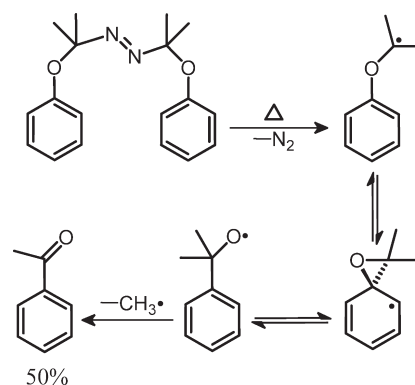


Figure 4. Example of O-neophyl rearrangement which proceeds from a C-centered radical to an O-centered radical.

ketone shown in Figure 4, the final cleavage leads to the loss of a methyl radical.

When this work has been already in progress, a report by Jones and co-workers revealed a conceptually elegant alternative approach to a radical O→C transposition.¹³ In this approach, photochemical excitation of 1-benzoyloxy-9,10-anthraquinone leads to the formation of 1-benzoyl-9,10-anthraquinone (44%). In contrast to the usual O-neophyl rearrangements, the energy cost for the formation of strained dearomatized three-membered intermediate is partially compensated by the coupling of the two radical centers and return to the ground state hypersurface. Unlike the terminating radical fragmentations described above,

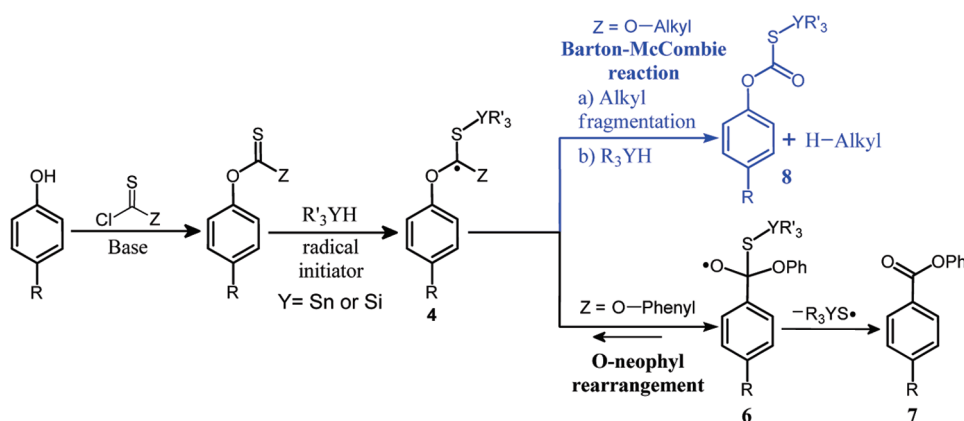


Figure 5. Rerouting Barton–McCombie reaction to the *O*-neophyl rearrangement pathway for the conversion of phenols into benzoate esters.

the rearranged carbonyl compound is furnished via a sequential epoxide ring-opening and alcohol oxidation. Thus far, the scope of this interesting transformation is limited to anthraquinones.

RESULTS AND DISCUSSION

In order to test the experimental feasibility of the proposed *O*-neophyl/fragmentation cascade, we decided to generate the aryloxy-substituted carbon radical **4** using the initial step of the Barton–McCombie deoxygenation reaction.¹⁴ This step involves selective addition of thiophilic Si- or Sn-centered radicals to the sulfur atom of thiocarbonyl (C=S) moiety. This choice not only assures that the appropriate carbon-centered radical is formed but also provides a weak C–S bond suitable for the equilibrium-shifting β -scission final step. Remarkably, the Barton–McCombie reaction has not been reported to provide such rearrangement products. Instead, this process is terminated by a fast C–O bond fragmentation forming an alkyl radical (path **4** \rightarrow **8**, Figure 5) and providing a synthetic connection between alcohols and alkanes. We hoped to divert the Barton–McCombie pathway and prevent the premature fragmentation step by replacing the alkyl group R with an aromatic substituent. Such a replacement provides a stronger C(sp²)–O bond and renders the putative sp²-radical product relatively unstable. We expected that if the fragmentation is sufficiently decelerated, the *O*-neophyl rearrangement of the aryl-substituted carbon radical **4** will become the major pathway.

Rearrangement of Thiocarbonates. The first test for our design was performed by treating diphenyl thiocarbonate with Bu₃SnH and AIBN in refluxing benzene. In this experiment, conversion was very low, and only a trace amount of the desired rearranged product (phenyl benzoate, **7**) was detected by ¹H NMR and GC. No improvement was observed when AIBN was replaced with other radical initiators such as benzoyl peroxide, V-40, and di-*tert*-butyl peroxide (TOOT) even upon heating with Bu₃SnH at 135 °C in a sealed tube. However, when triethylsilane (Et₃SiH)¹⁵ was used instead of Bu₃SnH, the proposed 1,2 O \rightarrow C transposition cascade did occur in the presence of TOOT at 135 °C in benzene with the formation of 59% of the phenyl benzoate product (path **4** \rightarrow **7**, Figure 5).

With the aim of expanding the scope of this process and gaining further insight into the mechanism, we examined substituent effects on the efficiency and selectivity of the new reaction. Diaryl thiocarbonates were synthesized in 75–90% yield from thiophosgene and the corresponding phenols. The results for the

rearrangements of substituted thiocarbonates agree with the proposed mechanism. For example, the observed similarity of the results for the radical stabilizing *p*-OMe and *p*-CN substituents (Table 1, entries 2–4) indicates the development of radical character in the migrating aryl group in the rate-limiting step.¹⁶ Not only higher yields ($\geq 80\%$) of rearranged benzoate esters were obtained for the *p*-OMe- and *p*-CN-substituted thiocarbonates, but we also observed 2–4:1 selectivity toward the formation of para-substituted benzoates (**7b**). Conversely, the rearrangement of fluoro- (entry 5) and pyridinyl-substituted (entry 8) thiocarbonates proceeded in lower yields and with lower selectivity. The correlation between reactivity and selectivity is consistent with the proposed mechanism (see Computational Analysis, *vide infra*). In a control experiment, *alkyl* aryl thiocarbonates were found to undergo complete fragmentation along the Barton–McCombie pathway under the same reaction conditions (entries 9 and 10, Table 1).

We also explored whether the diaryl thiocarbonates equipped with functional groups that are known to react under radical conditions can participate in more extended cascade transformations. Although nitro-substituted thiocarbonate (entry 7) gave a complicated reaction mixture, the reaction of the bromo derivative (entry 6) resulted in the formation of two compounds besides the rearranged esters **7a,b**(H,Br) (Figure 6). The new products were found to be the biphenyl derivatives of the rearranged products **11a** (12%) and **11b** (25%). The formation of these biphenyl compounds should proceed via the abstraction of bromine atom by the triethylsilyl radical (Et₃Si[•]) followed by radical aromatic substitution (RAS¹⁷) of the corresponding phenyl radical with benzene (solvent).

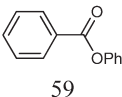
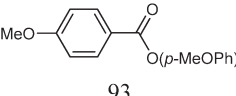
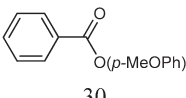
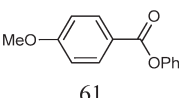
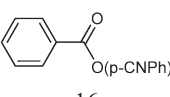
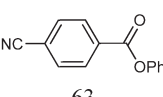
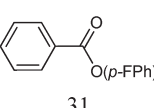
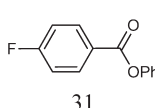
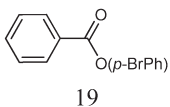
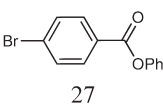
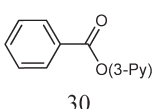
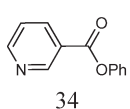
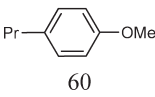
This transformation can occur either before or after *O*-neophyl rearrangement via path A or B, respectively (Figure 6). Although the two paths produce the same products, their yields and distributions would depend on the relative rate of the two alternative cascades, thus providing information on the rate of the cascade relative to the rate of Br atom abstraction from an aromatic molecule.

As is shown in Table 1, 3 equiv of Et₃SiH and 1.5 equiv of TOOT fully convert the Br-Ph thiocarbonate (entry 6) to products **7a,b**(H,Br) and **11a,b** in 4 h. When the relative amount of silane and initiator was decreased by 50%, the reaction initially produced only the rearranged aryl bromides **7a**(H,Br) (5%) and **7b**(H,Br) (8%) (15% conversion, 2 h, Table 2). Only upon additional heating was a small amount (6%) of biphenyls **11a** and **11b** formed (4 h, 50% conversion, 38% of **7b**(H,Br)/**7a**(H,Br)). These two experiments suggest that, at this concentration, addition to the thiocarbonyl moiety which initiates the *O*-neophyl

Table 1. Results of *O*-Neophyl Rearrangement/Fragmentation Reaction of Diaryl Thiocarbonates

$$\text{ArO}-\text{C}(=\text{S})-\text{OAr}' \xrightarrow[\text{PhH}]{\text{Et}_3\text{SiH (1.5 eq.)}, \text{TOOT (0.75 eq.)}} \text{Ar}-\text{C}(=\text{O})-\text{OAr}' + \text{Ar}'-\text{C}(=\text{O})-\text{OAr}$$

$$\text{9} \qquad \qquad \qquad \text{7a} \qquad \qquad \qquad \text{7b}$$

Entry	Ar	Ar'	Time (135°C)	Yield 7a [%]	Yield 7b [%]
1	Ph	Ph	2h	 59	NA
2	<i>p</i> -MeOPh	<i>p</i> -MeOPh	2h	 93	NA
3	Ph	<i>p</i> -MeOPh	2h	 30	 61
4	Ph	<i>p</i> -CNPh	1.5h	 16	 63
5	Ph	<i>p</i> -FPh	2h	 31	 31
6	Ph	<i>p</i> -BrPh ^{a, b}	4h	 19	 27
7	Ph	<i>p</i> -NO ₂ Ph	2-5h	^c	-
8	Ph	3-Pyridinyl ^a	4h	 30	 34
9	Ph	Et ^d	2h	^e	NA
10	Ph	3- <i>p</i> -MeOPh-propyl ^d	2h ^e	 60	NA

^a 3 equiv of Et₃SiH and 1.5 equiv of TOOT were used for full conversion of starting material. ^b Two additional products were formed besides 7a and 7b. ^c A complicated mixture was obtained. ^d TTMSS was used since no reaction was observed with Et₃SiH. ^e 100% alkyl fragmentation (Barton–McCombie).

rearrangement, cascade is >6 times faster than bromine abstraction and that path B is the major mechanism for the formation of 11a and 11b.

Since neither the intermediate product 10 nor the reduced products 12, 13 were detected, we tested whether 11a and 11b can be formed from 7a(H,Br) and 7b(H,Br) under the conditions of *O*-neophyl rearrangement (entry 5, Table 2). Indeed, 11a and 11b were the only new products observed in this experiment. This result provides further support for path B as the major pathway for the formation of these biphenyl compounds. The cascade can be driven completely toward the biphenyl products by greater excess of Et₃SiH and TOOT (69% of 11a + 11b from thiocarbonate 9(H,Br)).

Hence, these conditions can be used for carrying out the extended *O*-neophyl rearrangement/RAS cascade for the preparation of modified biphenyl compounds from the thiocarbonates of respective bromophenols.

The highest energy penalty for traveling along the *O*-neophyl potential energy surface is associated with the transient loss of aromaticity in the ipso-attack of the carbon radical 5 (Figure 3). It is reasonable to expect such an energy penalty to be significantly lower in polyaromatic compounds. For example, Schleyer and Pühlhofer reported that aromatic stabilization energy calculated via isomerization approach (isomerization stabilization energy, ISE)

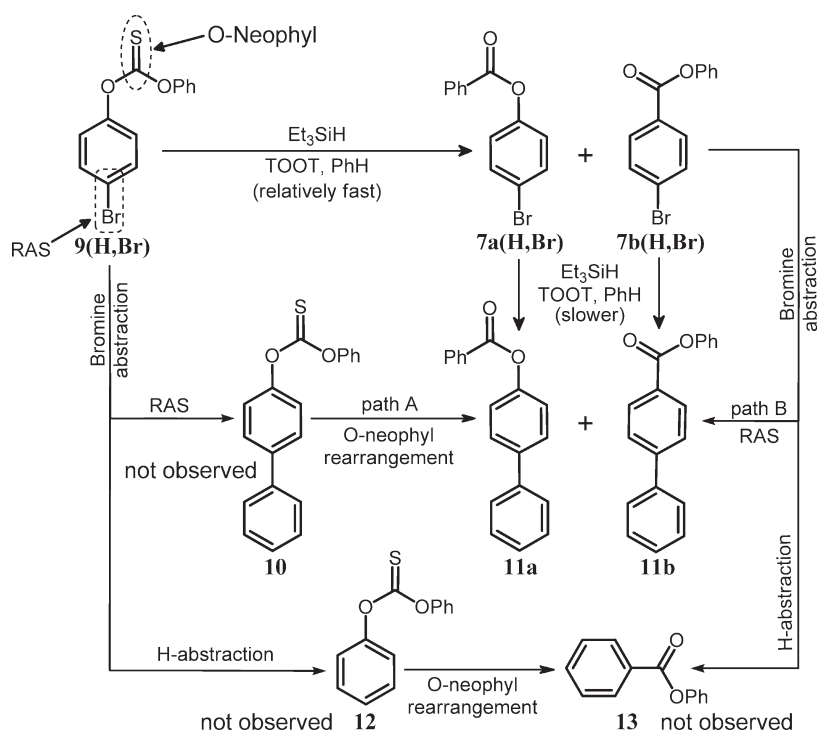


Figure 6. Coupled radical cascades in the reaction of bromo-substituted thiocarbonate **9(H,Br)** (entry 6, Table 1).

Table 2. Reaction of Bromothiocarbonate **9(H,Br)** with Varying Equivalents of Radical Reagents

entry	Et_3SiH (TOOT)	time (h)	yield (%)			
			7a(H,Br)	7a(H,Br)	11a	11b
1, 9(H,Br)	1.5 (0.75)	2 ^a	~5	~8	0	0
2, 9(H,Br)	1.5 (0.75)	4 ^b	14	24	2	4
3, 9(H,Br)	3 (1.5)	4	19	27	12	25
4, 9(H,Br)	4 (2)	10 ^c	0	0	21	48
5, (7a(H,Br) + 7b(H,Br)) (1:1.4)	6 (3)	3	18	17	14	28

^a 15% conversion of starting material. ^b 50% conversion of starting material. ^c Traces of phenyl benzoate were detected by NMR.

due to the formation of the second ring in naphthalene is ~ 14 – 15 kcal lower than ISE of benzene (B3LYP/6-311+G**).¹⁸

We have compared the energy cost for radical addition to benzene and polycyclic aromatics with B3LYP/6-31G** calculations. The differences are significant (Figure 7). Radical addition of a hydrogen atom to benzene is less exothermic than the addition to naphthalene (8 kcal/mol for the α -attack and 3 kcal/mol for the β -attack) and to phenanthrene (7–8 kcal/mol for the central ring attack). If the ipso-addition of stabilized carbon radicals follows the same trend and if *O*-neophyl rearrangement is a reversible process, one can expect the analogous rearrangement of phenyl polyaromatic thiocarbonates to be more selective.

Encouraged by these computational data, we investigated the reaction of polyaromatic thiocarbonates (entries 9–12). The reaction of 1-naphthylphenyl thiocarbonate (entry 1, Table 3) provides an ideal example of a completely selective and efficient *O*-neophyl rearrangement/fragmentation proceeding in $\sim 90\%$ yield. In a similar way, phenanthryl phenyl thiocarbonate undergoes the rearrangement exclusively at the phenanthryl moiety in 65% yield¹⁹ (entry 4, Table 3).

On the other hand, the reactions of β -substituted naphthyl and quinoyl thiocarbonates proceeded in lower yields and displayed

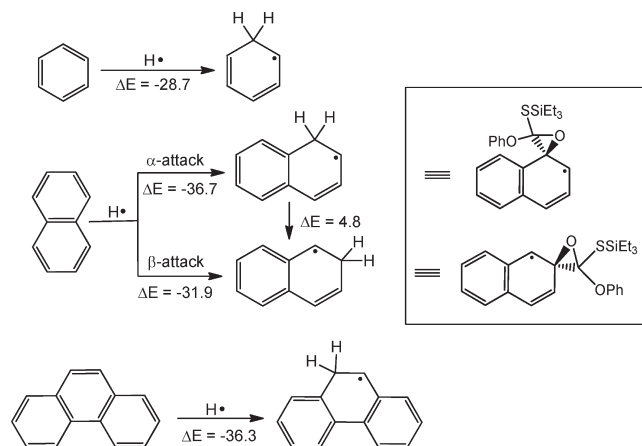


Figure 7. Difference between energy cost for dearomatization in benzene, naphthalene, and phenanthrene through H-radical addition (energies in kcal/mol, B3LYP/6-31G**).

only modest ~ 4 :1 regioselectivity. This observation is consistent with ~ 5 kcal/mol lower energy for the α -attack in Figure 7 and with

Table 3. Results of *O*-Neophyl Rearrangement/Fragmentation Reaction of Polyaromatic Thiocarbonates

Entry	Ar	Ar'	Time (135°C)	Yield 7a [%]	Yield 7b [%]
1	Ph	1-naphthyl	2h	 <1	 89
2	Ph	2-naphthyl	5h	 15	 61
3	Ph	6-quinoliny ^a	12h	 11	 40 ^{b, 19}
4	Ph	9-phenanthryl	4h	 0	 65 ^{b, 19}

^a 4 equiv of Et₃SiH and 2 equiv of TOOT were used for full conversion of starting material. ^b Several minor unidentified products were detected by NMR.

the well-known preference for the α -attack in naphthalene which is reproduced even at the Hückel level of theory.²⁰ Hence, it is clear that the position of the substituent in the polyaromatic system has a significant effect on the rearrangement efficiency and selectivity.

Rearrangement of Thiocarbonates. Thus far, we presented a method for the transformation of phenols into esters of the respective aromatic carboxylic acids. However, this process has one significant disadvantage. With the exception of several polyaromatic substrates, the unsymmetrical diaryl thiocarbonates show only modest selectivity. Thus, despite the high overall yields obtained for the benzoate esters, the synthetic value of this method is limited for unsymmetric thiocarbonates. Because the use of 2 equiv of a starting phenol can be impractical for expensive phenols, we continued to search for a more selective transformation which would increase the utility of the new reaction.

In contrast to the well-known fragmentation reaction of *O*-alkyl-substituted thiocarbonates (the Barton–McCombie reaction), the radical fragmentation of an *N*-alkyl group through the same process has not been reported in the literature (Figure 8a). Moreover, it has been shown that radical fragmentation of C–N bonds is inefficient. For instance, no scission of C–N bonds is observed in the radical racemization of chiral amines which occurs through a reversible abstraction of the α -hydrogen atom (Figure 8c).²¹ This observation is consistent with our computational analysis of the C–N bond radical fragmentation in a model thiocarbamate (Figure 8d). The calculated activation barrier of ~ 29 kcal/mol is

much higher than the literature barriers for *O*-neophyl rearrangements (vide infra).^{5a,11a,22,23} Encouraged by these results, we decided to change the *O*-alkyl substituent into an *N*-alkyl moiety and test whether the radical rearrangement of respective thiocarbonates is feasible (Figure 8b).

As the first step, we examined the reaction of *N,N*-diethyl-*O*-phenyl thiocarbamate (Figure 9a). To our disappointment, this compound remained unreactive even after 4 h at 135 °C in benzene in the presence of Et₃SiH (2equiv) and TOOT (1equiv) (Table 4, entry 1). We suggested that the lack of reactivity is due to the excessive stabilization of the anomeric radical by the hyperconjugative interaction with the adjacent nitrogen lone pair.²⁴ Thus, we have decided to moderate the nitrogen donor ability by attaching it to an aromatic group. By making this choice, we also intended to test whether *N*-aryl thiocarbonates could also react via a new *N*-neophyl rearrangement pathway (Figure 9b) analogous to the *O*-neophyl rearrangement.

Gratifyingly, the reaction of *N*-methyl-*N*-phenyl-*O*-(1-naphthyl) thiocarbamate afforded the corresponding amide as the only detectable product (Table 4, entry 2). Since low conversion was observed under the initial reaction conditions, we varied temperature, concentration, equivalents of reagents, and the nature of radical initiator. When the number of equivalents of Et₃SiH was increased to 4, the product yield improved to 68% (entries 2–4). A further small improvement of the amide yield (72%) was observed with 5 equiv of Et₃SiH (entry 5). Even better results were obtained when the TOOT was replaced with

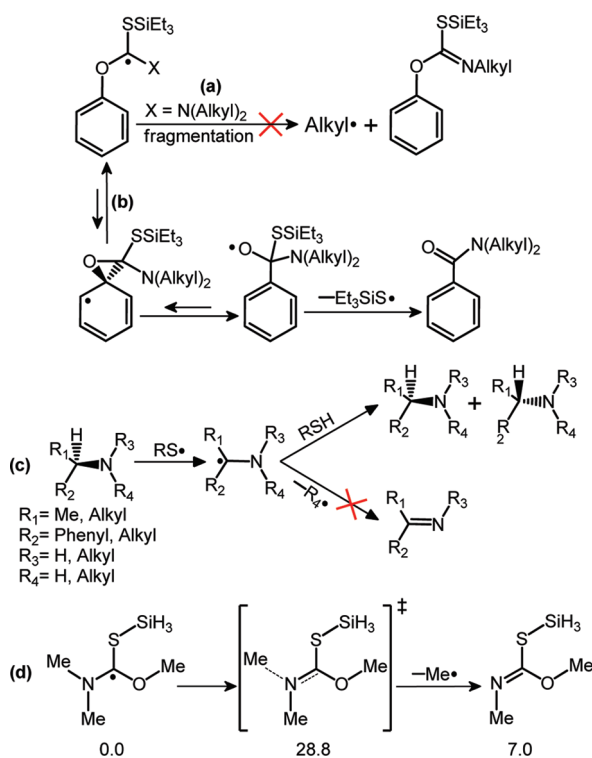


Figure 8. (a) Hypothetical C–N radical fragmentation through a Barton–McCombie-like mechanism. (b) Possible *O*-neophyl rearrangement of thiocarbamates. (c) Absence of C–N fragmentation during racemization of chiral amines through reversible H-abstraction by thyl radicals. (d) Model study of radical *N*-alkyl fragmentation in thiocarbamates at the UB3LYP/6-31+G** level (energies in kcal/mol).

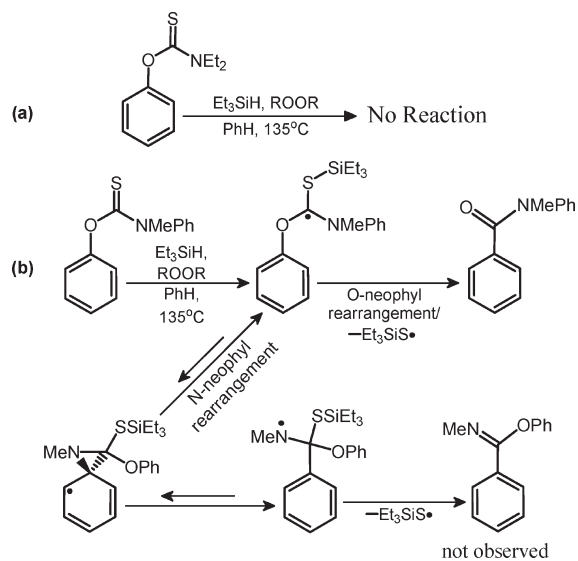


Figure 9. (a) Reaction of triethylsilyl radical with *N,N*-diethyl-*O*-phenyl thiocarbamate. (b) *O*-Neophyl vs *N*-neophyl rearrangement pathways in the reaction of thiocarbamates.

2,2-bis(*tert*-butylperoxy)butane (DTBPB). With this radical initiator, only 3 equiv of Et₃SiH was sufficient for obtaining 98% yield of the rearranged amide (entry 8).

Analogous to the results given in entry 6, both yield and conversion decreased at a higher concentration (entry 11). Clearly,

Table 4. Reaction Optimizations for the Rearrangement of Thiocarbamates^a

entry	Et ₃ SiH (equiv)	radical initiator	yield (%)	conv
1	2	TOOT	0	0
2	2	TOOT	17	48
3	3	TOOT	33	78
4	4	TOOT	68	100
5	5	TOOT	72	100
6 ^b	3	TOOT	~10	19
7	2	DTBPB	33	67
8	3	DTBPB	98	100
9 ^c	3	DTBPB	32	48
10 ^d	2	DTBPB	55	80
11 ^e	2	DTBPB	43	71
12 ^f	3	DTBPB	0	0

^a All entries are for *N*-methyl-*N*-phenyl-*O*-(1-naphthyl) thiocarbamate except for entry 1 which is for *N,N*-diethyl-*O*-phenyl thiocarbamate. Unless otherwise specified, all reactions were carried out at 11 mM of thiocarbamate, with a 1:2 molar ratio of radical initiator to Et₃SiH, at 135 °C for 4 h. ^b At 33 mM concentration of substrate. ^c 1:4 molar ratio of the radical initiator to Et₃SiH. ^d Reaction was run for 8 h. ^e At 22 mM concentration of substrate. ^f Reaction was run for 8 h at 100 °C.

the silicon radical addition to thiocarbonyl is not a rate-limiting step. The above results also suggest the presence of irreversible bimolecular termination reactions (Figure 10) which compete with the *O*-neophyl rearrangement pathway more efficiently at higher concentrations. Reaction with only 2 equiv of Et₃SiH (entry 10) or at a lower temperature (100 °C, entry 12) resulted in low or zero conversions even for the longer reaction times (8 h).

The proposed reaction sequence involves a formal transformation of the nucleophilic Et₃Si radical into an electrophilic (S-centered) Et₃SiS radical (Figure 10). Because the initiating and propagating radicals are different in nature, there is a possibility of polarity mismatch which could potentially render the overall cascade less efficient. We noticed the first indications that such effects may be important in our early experiments when initiation with a different source of Si radicals, tris-trimethylsilylsilane (TTMSS,¹⁵ Chatgililoglu's reagent), was tested. Although, in a few early attempts, we observed excellent yields and conversions, the process suffered from poor reproducibility, and in most of the cases, the reaction was extremely sluggish.²⁵

Polarity reversal catalysis has been used to facilitate chain propagation in radical processes, rendering them more efficient.²⁶ To test whether we can use this approach for the new cascade, we carried out TTMSS-promoted reactions in the presence of thiols. As shown in Table 5, the use of thiols (BuSH or PhSH) with TTMSS enables the formation of rearranged products. On the other hand, similar reactions with Et₃SiH were slower in the presence of thiols (not shown). These data suggest that a more detailed study of kinetic factors and their effect on the overall reaction efficiency is necessary in the future.

We applied the optimized rearrangement conditions (Table 4, entry 8) to a variety of thiocarbamates, readily available from thiophosgene, *N*-methyl aniline and the corresponding phenols in 75–97% isolated yields (Table 6). Since rearrangements of all thiocarbamates into amides proceeded in good to excellent yields, we have not attempted to optimize the reaction conditions for individual substrates.

In general, thiocarbamates with extended conjugation (entries 7–9) display higher reaction efficiency due to the greater stabilization of the radical character developed in the *O*-neophyl rearrangement step. Although, in contrast to the substituted thiocarbonates, the presence of radical-stabilizing CN and MeO groups (entries 2 and 3) does not further increase the yields of rearranged products (75–80%), most yields still compare favorably with the reactions of carbonates. Even though in a few cases the reaction yields are slightly lower, it is clear that the rearrangement of thiocarbamates provides a general solution to the problem of selectivity in radical *O*→*C* transposition. Since esters are compatible with the reaction conditions, this transformation provides a convenient approach to differentially substituted dicarboxylic acid derivatives (such as the ester amide in entry 8).

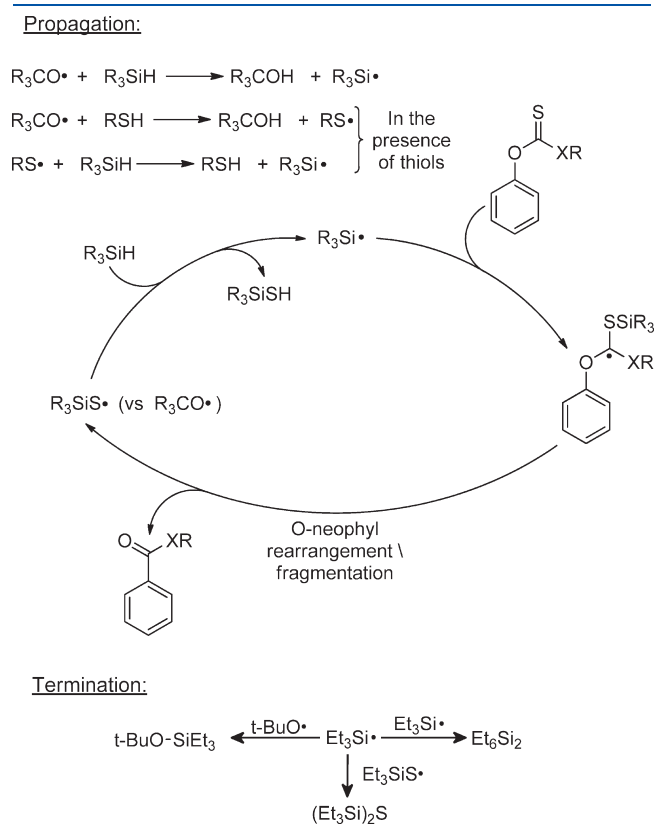


Figure 10. Possible propagation and termination steps of the radical cascade.

To test whether *N*-neophyl rearrangement is possible in the absence of *O*-neophyl pathway, we tested *N,N'*-dimethyl-*N,N'*-diphenylthiourea prepared from thiophosgene and *N*-methyl-*N*-phenylaniline and found it to be completely unreactive under the above optimized conditions. This result suggests that *N*-neophyl rearrangement should have a considerably higher activation barrier than the *O*-analogue.

The observed lack of 1,2 *N*→*C* transposition is noteworthy because a conceptually related 1,3 *N*→*C* transposition has been reported by Zard et al. in the radical Smiles rearrangement²⁷ of acetylaminopyridines.²⁸ In the latter case, the carbon-centered radical attacks the ipso-position via the formation of a four-membered spiro intermediate (Figure 11).²⁹

Computational Analysis. *Computational Procedures.* DFT calculations for the proposed reaction pathways utilized Gaussian 03 software.³⁰ All structures were fully optimized at the UB3LYP/6-31+G** level of theory, which is reported to provide an acceptable description of a number of radical reactions.³¹ All reactants, products, and intermediates were confirmed to be true minima by frequency calculations (zero negative frequencies). Each transition state had one imaginary frequency. Hyperconjugative radical stabilization energies were estimated using the natural bond orbital (NBO) method integrated in the Gaussian program.³²

Computational Results. The potential energy surfaces for possible *O*-neophyl rearrangements and fragmentation pathways as well as the computational analysis for selected substrates are summarized in Figures 12–14 and Table 7.

The calculations agree that the C–O bond scission (Barton-McCombie fragmentation) for alkyl substituted substrates (blue path) should be significantly faster than the *O*-neophyl rearrangement. The ~11 kcal/mol barrier difference explains why the *O*-neophyl cascade does not occur in those systems where the Barton-McCombie fragmentation pathway is available (entries 13 and 14, Table 1). On the other hand, the C–N bond scission (the hypothetical aza-Barton-McCombie fragmentation) is predicted to be much slower than the *O*-neophyl cascade. These results suggested that radical rearrangements of thiocarbamates may be more general and tolerate a greater variety of substituents at nitrogen.

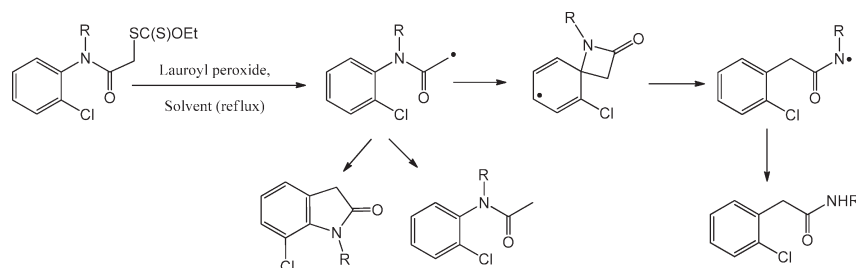
More detailed hypersurfaces for the rearrangements are presented in Figure 13. For both thiocarbonates and thiocarbamates, the first addition step of the silyl radical to the thiocarbonyl moiety is highly exothermic (18–24 kcal/mol) and has a low barrier of ~3 kcal/mol. However, the barrier for the subsequent *O*-neophyl rearrangement step is relatively high (21–25 kcal/mol). As the result, the *O*-neophyl pathway for the initially formed C-centered radical is kinetically competitive to the fragmentation back to the

Table 5. Testing the Effect of Thiols as Polarity Reversal Agents in the Rearrangement of Thiocarbonates and Thiocarbamates

	Peroxide	Silane	Entry	Thiol	Conversion (%)	Yield (%)	Time (h)
Ar=XR= <i>p</i> -MeOPh	TOOT	Et ₃ SiH	1	None	100	93	2
		TTMSS	2	None	NR	-	4
			3	0.01eq BuSH	68	45	4
Ar= 1-naphthyl XR= NMePh	DTBPB	Et ₃ SiH	4	-	100	98	4
		TTMSS	5	-	NR	-	3
			6	0.15eq BuSH	95	46	3
			7	0.15eq PhSH	86	47	3

Table 6. Results of *O*-Neophyl Rearrangement/Fragmentation Cascade of Thiocarbamates

Entry	Ar	Time (h)	Product	Yield [%]
1	Ph	4		88
2	<i>p</i> -MeOPh	4		80
3	<i>p</i> -CNPh	4		75
4	<i>p</i> -ClPh	4		63
5	<i>p</i> -MePh	4		72
6	<i>m</i> -MePh	4		76
7	<i>p</i> -PhPh	4		>99
8	<i>p</i> -(MeO ₂ C)Ph	4		97
9	1-naphthyl	4		98
10	2-naphthyl	3.5		77
11	6-quinolinyl	9		57

Figure 11. *N*→*C* transposition proceeding via a four-membered radical intermediate.

starting materials ($E_{-1}^{\ddagger} \sim 20\text{--}27$ kcal/mol, Figure 13 and Table 7). This competition lowers efficiency of the rearrangement

step and may account for the relatively high reaction temperature and excess of reagents needed for achieving complete conversions.

The barrier height for the *O*-neophyl rearrangement is consistent with previously calculated barriers for similar rearrangements of carbon radicals with different degrees of stabilization.^{5a,22} The relatively high value for the barrier stems from two factors: loss of aromatic stabilization in the TS/spiro-intermediate and effective stabilization of the carbon radical center in the reactant via interaction with the lone pairs of the three adjacent heteroatoms.³³ In our systems, steric repulsion exerted by the bulky OAr and SY groups

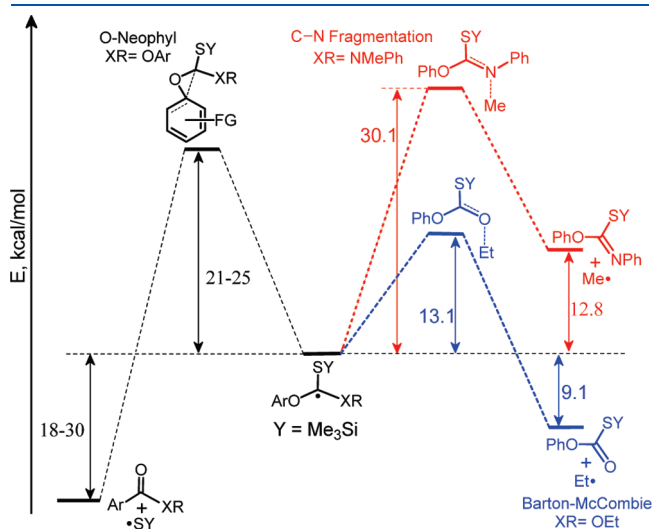


Figure 12. Comparison of potential energy surfaces for *O*-neophyl rearrangement in thiocarbonates and thiocarbamates with the C–O and C–N fragmentations at the UB3LYP/6-31+G** level (black path, *O*-neophyl rearrangement; blue path, Barton–McCombie fragmentation; red path, nitrogen analogue of Barton–McCombie fragmentation). (XR = OAr, NMePh; see Table 7 for different functional groups (FG)). Energies are in kcal/mol.

can raise the energy of the three-membered transition state (TS) as well.

Our calculations also provide the reason for the observed *O*-neophyl \gg *N*-neophyl selectivity in thiocarbamates. The calculated energy profile for the latter reaction is shown in Figure 13. The *N*-neophyl rearrangement pathway has an ~ 8 kcal/mol higher activation barrier, and the imidate product formation is 14 kcal/mol more endothermic than amide formation. Comparison with the calculated parameters for the N–C fragmentation (red path in Figure 12) illustrates that the *O*-neophyl rearrangement/C–S scission cascade represents the most kinetically and thermodynamically favored process among all three analyzed pathways in thiocarbamates.

Substituent Effects. The activation barriers of *O*-neophyl rearrangement are in good agreement with the experimental substituent effects for *para*-substituted thiocarbonates. As expected, radical-stabilizing groups (OMe and CN) lower the rearrangement barriers (Table 7, entries 2 and 3, respectively; Figure 14) at the substituted aromatic rings of phenyl aryl thiocarbonates, whereas the rearrangements at the phenyl groups in these compounds have the same activation barrier as in the parent diphenyl thiocarbonate (entry 1). Lower rearrangement barriers were also found for polyaromatic thiocarbonates (entries 7 and 8) where the penalty for the transient aromaticity loss is lower and resonance stabilization is higher. Encouragingly, the computational analysis predicts, in full agreement with the experimental data, that the rearrangements of phenyl thiocarbonates with 4-fluorophenyl, 4-bromophenyl, and 3-pyridinyl groups should have low selectivity. In a similar way, calculations also predict that thiocarbamates with radical-stabilizing groups should also have lower activation barriers for *O*-neophyl rearrangement (entries 11–14, Table 7). In thiocarbamates, however, the correlation between experimental yields of rearranged amides and the radical-stabilizing effect of substituents is less pronounced, suggesting that other factors and possible side reactions contribute to the overall reaction yield as well.

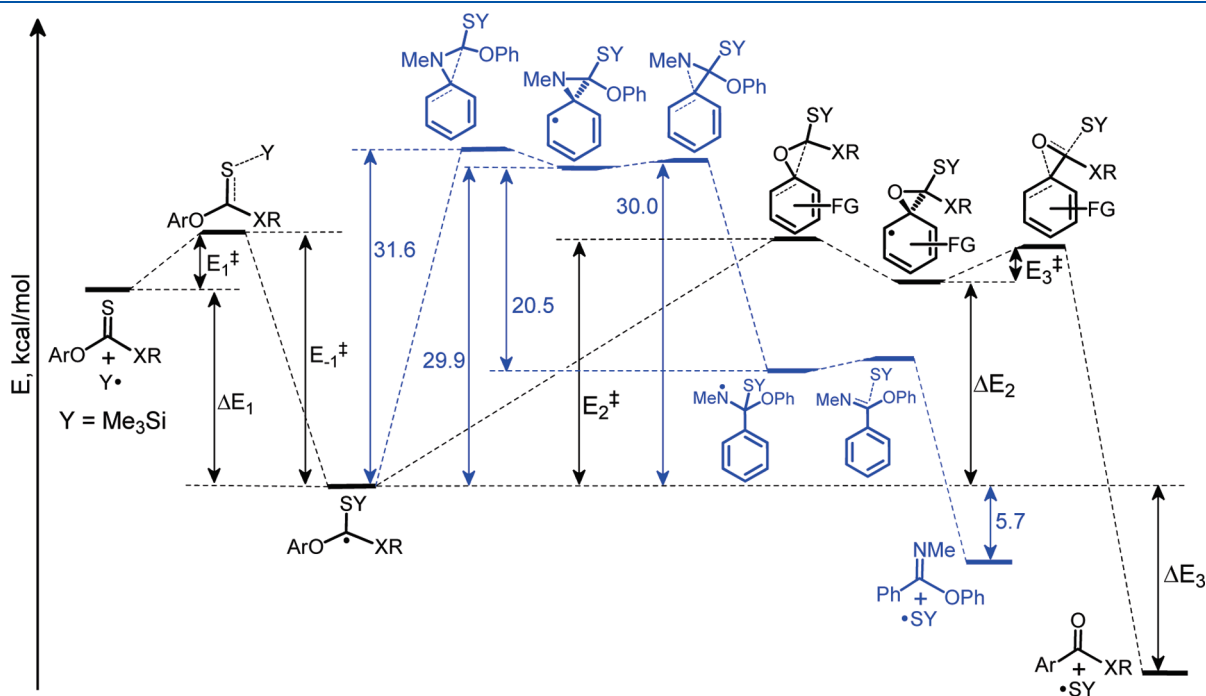


Figure 13. Potential energy surfaces for *O*-neophyl rearrangement (black) and the hypothetical *N*-neophyl rearrangement (blue) in thiocarbamates at the UB3LYP/6-31+G** level. Energies (kcal/mol) are summarized in Table 7.

Table 7. Summary of the Computational Results of the Rearrangement for Selected Diaryl-Substituted Thiocarbonates and Thiocarbamates at the UB3LYP/6-31+G Level^a**

entry	Ar	XR	E_1^\ddagger	E_{-1}^\ddagger	ΔE_1	E_2^\ddagger	ΔE_2	E_3^\ddagger	ΔE_3
1	Ph	OPh	3.2	26.3	-23.1	24.8			-26.7
2	Ph	O-(<i>p</i> -MeOPh)	3.1	25.4	-22.3	24.4			-27.3
	<i>p</i> -MeOPh	OPh				23.9			-29.3
3	Ph	O-(<i>p</i> -CNPh)	3.0	27.5	-24.5	24.9			-25.9
	<i>p</i> -CNPh	OPh				23.2	17.2		-23.7
4	Ph	O-(<i>p</i> -FPh)	3.3	26.2	-22.9	24.5			-27.0
	<i>p</i> -FPh	OPh				24.4			-27.8
5	Ph	O-(<i>p</i> -BrPh)	3.3	27.0	-23.7	24.4			-26.5
	<i>p</i> -BrPh	OPh				24.1			-27.0
6	Ph	O-(3-pyridinyl)	3.2	25.7	-23.5	24.9			-26.8
	3-pyridinyl	OPh				24.5			-26.6
7	Ph	O-(1-naphthyl)	2.6	24.1	-21.5	22.7			-28.3
	1-naphthyl	OPh				21.0	13.4	0.6	-25.7
8	Ph	O-(2-naphthyl)	3.1	24.7	-21.6	22.7			-29.0
	2-naphthyl	OPh				21.4			-29.1
9	Ph	OEt	4.5	23.2	-18.7	22.0			-30.0
10	Ph	NMePh	2.8	20.9	-18.1	23.1			-19.4
11	<i>p</i> -MeOPh	NMePh	3.0	20.5	-17.5	22.3			-21.2
12	<i>p</i> -CNPh	NMePh	2.4	21.6	-19.2	20.9	19.9	0.3	-17.7
13	<i>p</i> -MeO ₂ CPh	NMePh	2.4	21.5	-19.1	21.4	20.2	0.1	-17.9
14	1-naphthyl	NMePh	2.6	21.2	-18.6	21.2	17.2	0.9	-18.5

^a Energies are given in kcal/mol.

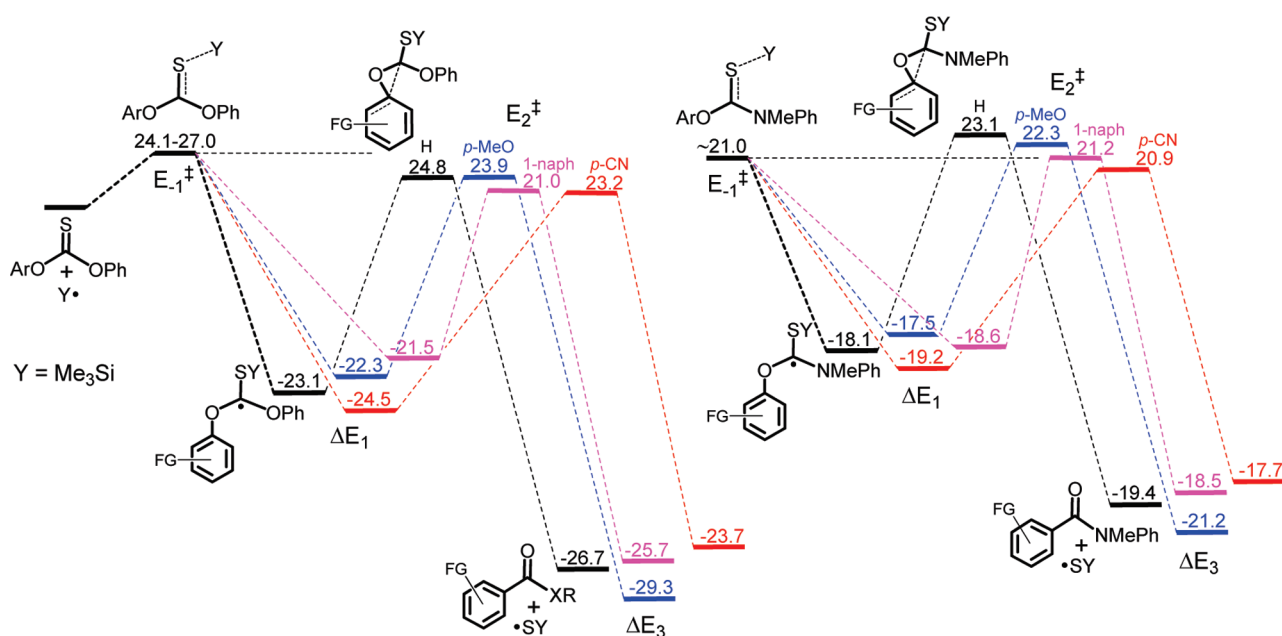


Figure 14. Comparison between reaction energies of *O*-neophyl rearrangement and retroradical fragmentation in substituted thiocarbonates and thiocarbamates (energies in kcal/mol).

Several considerable differences between *O*-neophyl rearrangement of thiocarbonates and thiocarbamates are demonstrated in Figure 14. First, the rearrangement of thiocarbonates includes more exothermic addition and fragmentation steps than the rearrangement of thiocarbamates. Second, lower activation barriers (E_{-1}^\ddagger) were found for the retro-fragmentation of carbon radicals produced from thiocarbamates. Although the rearrangement

barriers for thiocarbonates are generally higher than those for thiocarbamates, they are always lower than the barriers for the retro step (E_{-1}^\ddagger). Together, the computational data suggest a less efficient *O*-neophyl rearrangement in the case of thiocarbamates, which explains why longer reaction time and higher equivalents of radical reagents were needed for complete conversion of these substrates. This trade-off in the efficiency of the

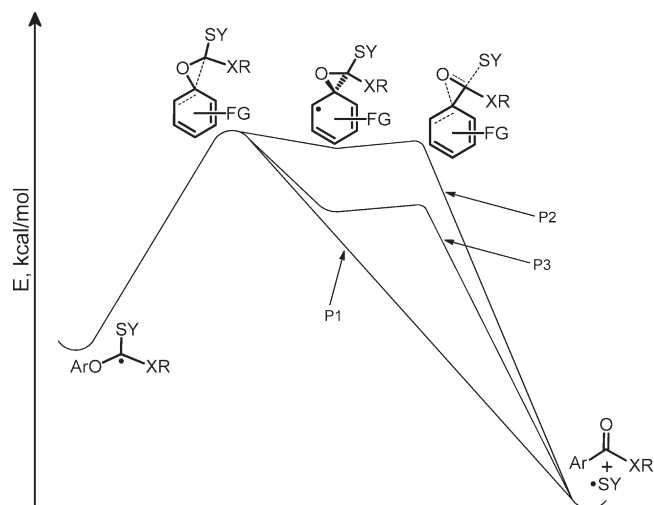


Figure 15. Concerted (P1) and shallow nonconcerted (P2 and P3) potential energy surfaces for *O*-neophyl rearrangement.

rearrangement step is, however, compensated by the high selectivity of the *O*-neophyl rearrangement in thiocarbonates.

Earlier computational^{5a,22} and experimental³⁴ studies suggested that *O*-neophyl rearrangement usually proceeds via a three-membered dearomatized radical intermediate. Interestingly, in our systems where the rearrangement is coupled with fragmentation, the DFT calculations suggest a concerted pathway for the *O*-neophyl rearrangement. The three-membered intermediate could not be located for most of the substrates at the UB3LYP/6-31+G** energy surface. Instead, all attempts for their structural optimizations led to the final rearranged/fragmented products (ester or amide + YS^\bullet , P1, Figure 15). Only in the case of systems where higher radical stability is provided through extended conjugation (entries 3, 7, 12–14; Table 7) could minima for the three-membered radical intermediates be located. However, even in those cases the calculated barrier ($E_3^\ddagger < 1$ kcal/mol) for the following ring-opening is extremely low. No other intermediates are located because the ring-opening is accompanied by the final C–S bond scission, directly affording the C=O bond in the final product. Therefore, the barrier of the ring-opening/fragmentation step is insignificant, and even when a minimum for the three-membered radical intermediate is located (entries 3, 7 and 14; P3), the reaction path still follows a very shallow potential energy surface (entries 12 and 13, Table 7; P2, Figure 15). A similar situation has been observed for the *N*-neophyl rearrangement pathway where the difference between the three-membered intermediate and earlier TS is less than 1 kcal/mol (Figure 13, Table 7). No 3-membered radical intermediate was located for the 2-naphthyl thiocarbonate moiety, suggesting that it is less stable than the corresponding 1-naphthyl thiocarbonate 3-membered intermediate.

CONCLUSION

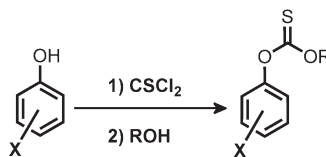
We have designed an efficient 1,2 $\text{O}\rightarrow\text{C}$ radical transposition/fragmentation cascade for the transformation of phenols into benzoates and benzamides. This process can be used as an alternative to metal catalyzed carbonylation of aromatic triflates. Our computational studies fully rationalize the moderate rearrangement selectivity for diaryl thiocarbonates and high selectivity for diaryl thiocarbonates. We have shown that, out of many possible pathways, *O*-neophyl rearrangement is the most kinetically and

thermodynamically favorable direction. In addition, the calculated activation barrier for *N*-neophyl rearrangement is relatively high, which explains the absence of this reaction in the literature. Overall, in accord with our initial design, the reaction cascade is driven by the high exothermicity (37–50 kcal/mol below the initial reactants) of the last equilibrium shifting fragmentation step.

EXPERIMENTAL SECTION

General Information. All NMR spectra were collected at 400 MHz for ^1H NMR and 100 MHz for ^{13}C NMR using CDCl_3 as solvent. Infrared (IR) spectroscopy was performed using a nitrogen-purged FTIR spectrometer.

- 1) X = H, R = Ph
- 2) X = *p*-MeO, R = *p*-MeOPh
- 3) X = H, R = *p*-MeOPh
- 4) X = H, R = *p*-CNPh
- 5) X = H, R = *p*-FPh
- 6) X = H, R = *p*-BrPh
- 7) X = H, R = *p*-NO₂Ph
- 8) X = H, R = 3-Pyridinyl
- 9) X = H, R = Et
- 10) X = H, R = 3-(4-MeOPh)Pr
- 11) X = H, R = 1-naphthyl
- 12) X = H, R = 2-naphthyl
- 13) X = H, R = 6-quinolinyl
- 14) X = H, R = 9-phenanthryl



General Procedure for the Synthesis of Symmetrical Thiocarbonates. Phenol (2.4 mmol) was dissolved in 8 mL of aqueous 0.3 M NaOH and added to a solution of CSCl_2 (1.2 mmol) in 10 mL of CH_2Cl_2 . The reaction solution (two layers) was stirred vigorously for 2 h and then diluted with CH_2Cl_2 , washed with brine, and dried with Na_2SO_4 . Solvent was removed under reduced pressure, and the crude mixture was purified by column chromatography to afford the corresponding thiocarbonate.

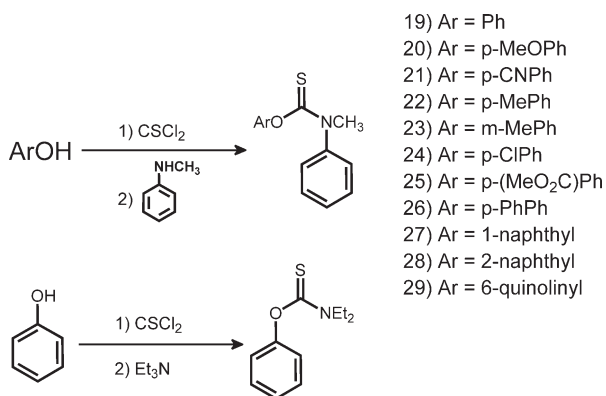
General Procedures for the Synthesis of Nonsymmetrical Thiocarbonates. *Procedure A.* The first phenol (1.2 mmol) was dissolved in 4 mL of aqueous 0.3 M NaOH and added to a 10 mL of a CH_2Cl_2 solution of CSCl_2 (1.8 mmol). The two layers were stirred vigorously for 1 h. The reaction mixture was diluted with CH_2Cl_2 and washed with brine. The organic layers were combined and dried with Na_2SO_4 , and solvent and excess CSCl_2 were removed under reduced pressure. The reaction mixture was then redissolved in 10 mL of CH_2Cl_2 . The second phenol (1.2 mmol) was then dissolved in 4 mL of 0.3 M NaOH_{aq}, added to the above CH_2Cl_2 solution of the reaction mixture, and stirred for 2 h. The reaction was then worked up in the same way as before and purified by column chromatography to afford the corresponding thiocarbonate.

Procedure B. The first phenol (1.2 mmol) and CSCl_2 (1.8 mmol) were dissolved in 10 mL of CH_2Cl_2 and stirred at 0 °C. Neat pyridine (1.5 mmol) was then added dropwise at 0 °C. The reaction mixture was allowed to warm to room temperature for 15 min upon stirring, diluted with CH_2Cl_2 , and washed with brine. The organic layers were combined and dried with Na_2SO_4 . Solvent and excess CSCl_2 were removed under reduced pressure. The reaction mixture and the second phenol (1.2 mmol) were dissolved in 10 mL of CH_2Cl_2 and stirred at room temperature. Neat pyridine (1.5 mmol) was added dropwise to the reaction mixture at room temperature. The reaction mixture was stirred for 30 min, worked up in the same way as above, and purified by column chromatography to afford the corresponding thiocarbonate.

Procedure C. The aryl alcohol (1.2 mmol) and PhOCsCl (1.8 mmol) were dissolved in 10 mL of CH_2Cl_2 or MeCN. CsF–Celite (2.4 mmol) was then added to form a heterogeneous mixture. The reaction mixture

was stirred at room temperature for 2–6 h and monitored by TLC. Then reaction mixture was diluted with CH_2Cl_2 and washed with brine. The organic layers were combined and dried with Na_2SO_4 , and solvent was removed under reduced pressure. The crude mixture was purified by column chromatography to afford the corresponding thiocarbonate.

General Procedures for the Synthesis of Thiocarbonates.



Procedure D. The phenol (1.2 mmol) was dissolved in 4 mL of aqueous 0.3 M NaOH and added to a 10 mL CH_2Cl_2 solution of CSCl_2 (1.8 mmol). The two layers were stirred vigorously for 1 h. The reaction mixture was diluted with CH_2Cl_2 and washed with brine. The organic layer was dried with Na_2SO_4 , and solvent and excess CSCl_2 were removed under reduced pressure. The reaction mixture was then redissolved in 10 mL of CH_2Cl_2 . Neat *N*-methylaniline (2.4 mmol) was then added to the above CH_2Cl_2 solution of the reaction mixture and stirred for 10 min. The reaction was then diluted with CH_2Cl_2 and washed with brine followed by 10 mL of 0.1 N HCl_{aq} . The organic layer was dried with Na_2SO_4 . Solvent was removed under reduced pressure, and the crude mixture was purified by column chromatography to afford the corresponding thiocarbonate.

Procedure E. The phenol (1.2 mmol) and CSCl_2 (1.8 mmol) were dissolved in 10 mL of CH_2Cl_2 and stirred at 0 °C. Neat pyridine (1.5 mmol) was then added dropwise at 0 °C. The reaction mixture was allowed to warm to room temperature for 15 min upon stirring, diluted with CH_2Cl_2 , and washed with brine. The organic layer was dried with Na_2SO_4 . Solvent and excess CSCl_2 were removed under reduced pressure. The reaction mixture was dissolved in 10 mL of CH_2Cl_2 and stirred at room temperature. Neat *N*-methylaniline (2.4 mmol) was then added to the above CH_2Cl_2 solution of the reaction mixture and stirred for 10 min. The reaction was then diluted with CH_2Cl_2 , washed with brine followed by 20 mL of 0.1 N HCl_{aq} , and dried with Na_2SO_4 . Solvent was removed under reduced pressure, and the obtained crude mixture was purified by column chromatography to afford the corresponding thiocarbonate.

Procedure F. The aryl alcohol (1.2 mmol) and $\text{Ph}(\text{Me})\text{NCSCl}$ (1.8 mmol) were dissolved in 10 mL of CH_2Cl_2 or EtOAc. Et_3N (2.4 mmol) was then added, and reaction mixture was stirred at room temperature (or at reflux) for 12 h and monitored by TLC. Then reaction mixture was diluted with CH_2Cl_2 or EtOAc and washed with brine. The organic layers were combined and dried with Na_2SO_4 , and solvent was removed under reduced pressure. The crude mixture was purified by column chromatography to afford the corresponding thiocarbonate.

Ph(Me)NCSCl. *N*-Methylaniline (3 mmol) was dissolved in 10 mL of CH_2Cl_2 and added dropwise to a 5 mL CH_2Cl_2 solution of CSCl_2 (1.5 mmol) at 0 °C. Then reaction mixture was diluted with CH_2Cl_2 and washed with brine. The organic layers were combined and dried with Na_2SO_4 , and solvent was removed under reduced pressure. The crude mixture was directly used in the preceding synthesis step.

General Procedure for the *O*-Neophyl Rearrangement/Fragmentation Reaction. Et_3SiH and TOOT were added to a benzene solution of the starting thiocarbonate or thiocarbonate.

The solution was then purged with N_2 for 15 min, sealed in an Ace Glass pressure tube or thick-walled Pyrex tube, and heated at 135 °C in an oil bath. Solvent was evaporated, and product was purified by chromatography.

General Procedure for the Synthesis of Aryl Benzoates.

Phenol (0.214 mmol) and benzoyl chloride (0.221 mmol) were dissolved in 6 mL of DCM/ Et_3N (5:1) mixture and stirred for 1 h. The reaction solution was diluted with DCM, washed with brine, dried with Na_2SO_4 , and then dried under reduced pressure. The crude reaction mixture was purified by column chromatography.

***O,O*-Bis(4-methoxyphenyl) thiocarbonate (2):** white solid; mp 161–163 °C; 76%; ^1H NMR (400 MHz, CDCl_3) δ 7.07 (4H, d, J = 9.1 Hz), 6.89 (4H, d, J = 9.1 Hz), 3.77 (6H, s); ^{13}C NMR (100 MHz, CDCl_3) δ 196.1, 158.0, 147.4, 122.7, 114.7, 55.7; IR (KBr) 3051, 2960, 2837, 1883, 1780, 1646, 1601, 1512, 1501, 1456, 1301, 1270, 1244, 1184, 1100, 1035 cm^{-1} ; HRMS (EI+) calcd for $\text{C}_{15}\text{H}_{14}\text{O}_4\text{S}$ 290.06128, found 290.06040.

***O*-(4-Methoxyphenyl)-*O*-phenyl thiocarbonate (3):** procedure A; white solid; mp 109–111 °C; 81%; ^1H NMR (400 MHz, CDCl_3) δ 7.47 (2H, t, J = 7.5 Hz), 7.33 (1H, m), 7.23 (2H, m), 7.15 (2H, d, J = 9.1 Hz), 6.96 (2H, d, J = 9.1 Hz), 3.83 (3H, s); ^{13}C NMR (100 MHz, CDCl_3) δ 195.6, 158.1, 153.8, 147.4, 129.8, 127.0, 122.7, 122.0, 114.7, 55.7; IR (KBr) 3051, 2958, 2837, 1882, 1591, 1507, 1489, 1455, 1300, 1282, 1259, 1241, 1181, 1099, 1068, 1035, 1001 cm^{-1} ; HRMS (EI+) calcd for $\text{C}_{14}\text{H}_{12}\text{O}_3\text{S}$ 260.05072, found 260.05061.

***O*-(4-Cyanophenyl)-*O*-phenyl thiocarbonate (4):** procedure A; white solid; mp 157–159 °C; 75%; ^1H NMR (400 MHz, CDCl_3) δ 7.77 (2H, d, J = 8.8 Hz), 7.48 (2H, t, J = 7.6 Hz), 7.35 (3H, m), 7.22 (2H, m); ^{13}C NMR (100 MHz, CDCl_3) δ 193.7, 156.3, 153.5, 134.1, 130.0, 127.3, 123.6, 121.8, 118.1, 111.2; IR (KBr) 3096, 3056, 2923, 2234, 1598, 1504, 1491, 1455, 1409, 1284, 1264, 1234, 1209, 1196, 1156, 1103, 1067 cm^{-1} ; HRMS (EI+) calcd for $\text{C}_{14}\text{H}_9\text{O}_2\text{NS}$ 255.03540, found 255.03449.

***O*-(4-Fluorophenyl)-*O*-phenyl thiocarbonate (5):** procedure A; white solid; mp 108–112 °C; 78%; ^1H NMR (400 MHz, CDCl_3) δ 7.48 (2H, t, J = 7.5 Hz), 7.34 (1H, m), 7.3–7.1 (6H, m); ^{13}C NMR (100 MHz, CDCl_3) δ 194.8, 160.8 (d, J = 244.6 Hz), 153.5, 149.3, 129.7, 126.9, 123.3 (d, J = 8.6 Hz), 121.7, 116.3 (d, J = 23.7 Hz); IR (KBr) 3072, 3050, 1888, 1653, 1614, 1598, 1506, 1491, 156, 1415, 1290, 1278, 1243, 1176, 1147, 1088, 1068, 1002, 931, 911, 845, 827, 810, 776, 757, 738, 709, 695, 626, 603, 506, 492 cm^{-1} ; HRMS (EI+) calcd for $\text{C}_{13}\text{H}_9\text{O}_2\text{SF}$ 248.03073, found 248.03009.

***O*-(4-Bromophenyl)-*O*-phenyl thiocarbonate (6):** procedure A; white solid; mp 134–136 °C; 81%; ^1H NMR (400 MHz, CDCl_3) δ 7.58 (2H, d, J = 8.9 Hz), 7.47 (2H, t, J = 7.4 Hz), 7.34 (1H, m), 7.22 (2H, m), 7.12 (2H, d, J = 8.9 Hz); ^{13}C NMR (100 MHz, CDCl_3) δ 194.5, 153.7, 152.6, 132.9, 129.9, 127.1, 123.9, 121.9, 120.3; IR (KBr) 3071, 3050, 2919, 2850, 1948, 1899, 1878, 1746, 1661, 1598, 1485, 1456, 1397, 1376, 1309, 1283, 1244, 1231, 1209, 1191, 1164, 1093, 1067, 1014, 1002, 931, 913, 938, 795, 775, 722, 704, 691, 633, 611, 540, 494, 411, 403 cm^{-1} ; HRMS (EI+) calcd for $\text{C}_{13}\text{H}_9\text{O}_2\text{SBr}$ 307.95066, found 307.95011.

***O*-(4-Nitrophenyl)-*O*-phenyl thiocarbonate (7):** procedure A; white solid; mp 158–162 °C; 74%; ^1H NMR (400 MHz, CDCl_3) δ 8.35 (2H, d, J = 9.1 Hz), 7.48 (2H, m), 7.41 (2H, d, J = 9.1 Hz), 7.36 (1H, m), 7.23 (2H, m); ^{13}C NMR (100 MHz, CDCl_3) δ 193.6, 157.7, 153.5, 146.3, 130.0, 127.3, 125.6, 123.4, 121.8; IR (KBr) 3076, 1614, 1592, 1529, 1487, 1456, 1353, 1288, 1269, 1245, 1155, 1098, 1066, 1013, 1002 cm^{-1} ; HRMS (EI+) calcd for $\text{C}_{13}\text{H}_9\text{O}_4\text{NS}$ 275.02523, found 275.02455.

***O*-Phenyl-*O*-3-pyridinyl thiocarbonate (8):** procedure B; white solid; mp 94–97 °C; 75%; ^1H NMR (400 MHz, CDCl_3) δ 8.58 (1H, dd, J = 1.2, 4.8 Hz), 8.56 (1H, d, J = 2.6 Hz), 7.59 (1H, ddd, J = 1.4, 2.8, 8.3 Hz), 7.48 (2H, m), 7.42 (1H, ddd, J = 0.3, 4.8, 8.3 Hz), 7.35 (1H, m), 7.23 (2H, m); ^{13}C NMR (100 MHz, CDCl_3) δ 194.4, 153.6, 150.3, 147.9, 144.0, 130.0, 129.9, 127.2, 124.2, 121.8; IR (KBr) 3053, 1875, 1590,

1492, 1478, 1457, 1428, 1371, 1321, 1310, 1282, 1267, 1249, 1193, 1160, 1097, 1071, 1038, 1023, 1002 cm^{-1} ; HRMS (EI+) calcd for $\text{C}_{12}\text{H}_9\text{O}_2\text{NS}$ 232.04322 $[\text{M} + \text{H}]^+$, found 232.04126 $[\text{M} + \text{H}]^+$.

O-Ethyl-*O*-phenyl thiocarbonate (**9**): procedure A; colorless oil, 89%; ^1H NMR (400 MHz, CDCl_3) δ 7.42 (2H, t, $J = 7.6$ Hz), 7.29 (1H, t, $J = 7.3$ Hz), 7.11 (2H, d, $J = 7.7$ Hz), 4.60 (2H, q, $J = 7.1$ Hz), 1.47 (3H, t, $J = 7.1$ Hz); ^{13}C NMR (100 MHz, CDCl_3) δ ; IR (KBr) 3058, 3043, 2984, 2937, 2904, 2870, 2491, 2410, 1942, 1864, 1762, 1733, 1675, 1593, 1490, 1464, 1457, 1398, 1372, 1282, 1191, 1155, 1095, 1061, 1044, 1023, 1004 cm^{-1} ; HRMS (EI+) calcd for $\text{C}_9\text{H}_{10}\text{O}_2\text{S}$ 182.04015, found 182.03956.

O-[3-(4-Methoxyphenyl)propyl]-*O*-phenyl thiocarbonate (**10**): procedure A; colorless oil, 58%^p ^1H NMR (400 MHz, CDCl_3) δ 7.43 (2H, t, $J = 7.5$ Hz), 7.30 (1H, t, $J = 7.4$ Hz), 7.13 (4H, m), 6.86 (2H, d, $J = 8.6$ Hz), 4.54 (2H, t, $J = 6.4$ Hz), 3.80 (3H, s), 2.73 (2H, t, $J = 7.3$ Hz), 2.12 (2H, m); ^{13}C NMR (100 MHz, CDCl_3) δ 195.2, 158.0, 153.4, 132.8, 129.5, 129.3, 126.5, 121.9, 113.9, 73.6, 55.3, 31.1, 30.0; IR (KBr) 3060, 3031, 2996, 2953, 2834, 2488, 1881, 1781, 1612, 1590, 1513, 1490, 1456, 1389, 1359, 1291, 1246, 1201, 1112, 1070, 1037, 1021, 1004 cm^{-1} ; HRMS (EI+) calcd for $\text{C}_{17}\text{H}_{18}\text{O}_3\text{S}$ 302.09767, found 302.09717.

O-(1-Naphthyl)-*O*-phenyl thiocarbonate (**11**): procedure A; white solid; mp 59–61 °C; ^1H NMR (400 MHz, CDCl_3) δ 8.03 (1H, d, $J = 8.2$ Hz), 7.94 (1H, d, $J = 7.7$ Hz), 7.85 (1H, d, $J = 8.2$ Hz), 7.6–7.5 (5H, m), 7.41 (1H, d, $J = 7.5$ Hz), 7.36 (1H, t, $J = 7.4$ Hz), 7.31 (2H, d, $J = 7.9$ Hz); ^{13}C NMR (100 MHz, CDCl_3) δ 194.7, 153.8, 149.5, 134.9, 129.9, 128.4, 127.2, 127.1, 127.0, 126.9, 126.5, 122.0, 121.3, 118.8; IR (KBr) IR (KBr) 3062, 2921, 2850, 2459, 1936, 1600, 1591, 1509, 1490, 1457, 1392, 1277, 1194, 1153, 1079, 1042, 1014, 1003, 921, 860, 844, 799, 770, 737, 688, 658, 604, 555, 482, 433, 410 cm^{-1} ; HRMS (EI+) calcd for $\text{C}_{17}\text{H}_{12}\text{O}_2\text{S}$ 280.05580, found 280.05450.

O-(2-Naphthyl)-*O*-phenyl thiocarbonate (**12**): procedure A; white solid; mp 134–136 °C; 84%; ^1H NMR (400 MHz, CDCl_3) δ 7.91 (1H, d, $J = 8.92$ Hz), 7.86 (2H, m), 7.66 (1H, d, $J = 2.28$ Hz), 7.48 (4H, m), 7.37 (1H, dd, $J = 2.36, 8.88$ Hz), 7.32 (1H, m), 7.26 (2H, m); ^{13}C NMR (100 MHz, CDCl_3) δ 194.89, 153.58, 151.04, 133.66, 131.85, 129.68, 127.92, 127.86, 126.84, 126.82, 126.26, 121.82, 121.02, 118.95; HRMS (EI+) calcd for $\text{C}_{17}\text{H}_{12}\text{O}_2\text{S}$ 280.05580, found 280.05526.

O-(6-Quinoliny)-*O*-phenyl thiocarbonate (**13**): procedure C; white solid; mp 139–141 °C; 54%; ^1H NMR (400 MHz, CDCl_3) δ 8.94 (1H, dd, $J = 1.6, 4.2$ Hz), 8.19 (2H, m), 7.66 (1H, d, $J = 2.56$ Hz), 7.62 (1H, dd, $J = 2.64, 9.08$ Hz), 7.45 (3H, m), 7.33 (1H, m), 7.25 (2H, m); ^{13}C NMR (100 MHz, CDCl_3) δ 194.6, 153.5, 151.0, 150.6, 146.5, 136.0, 131.3, 129.7, 128.5, 126.9, 124.8, 121.8, 121.7, 118.9; HRMS (ESI+) calcd for $\text{C}_{16}\text{H}_{11}\text{O}_2\text{NS}$ 282.05887 $[\text{M} + \text{H}]^+$, found 282.05879 $[\text{M} + \text{H}]^+$.

O-(1-Phenanthryl)-*O*-phenyl thiocarbonate (**14**): procedure C; yellow solid; mp 96–98 °C; 79%; ^1H NMR (400 MHz, CDCl_3) δ 8.70 (1H, dd, $J = 1.92, 6.76$ Hz), 8.65 (1H, d, $J = 8.04$ Hz), 8.06 (1H, m), 7.88 (1H, d, $J = 7.68$ Hz), 7.72–7.57 (4H, m), 7.44 (2H, m), 7.30 (3H, m), 7.21 (1H, m); ^{13}C NMR (100 MHz, CDCl_3) δ 194.4, 153.7, 147.8, 131.7, 131.3, 129.8, 129.7, 128.7, 127.5, 127.3, 127.2, 127.0, 126.9, 125.9, 123.2, 122.8, 121.9, 121.8, 118.5; HRMS (EI+) calcd for $\text{C}_{21}\text{H}_{14}\text{O}_2\text{S}$ 330.07145, found 330.07140.

p-Fluorophenyl benzoate (**15**): (synthesized from benzoyl chloride) white solid; mp 48–50 °C; 97%; ^1H NMR (400 MHz, CDCl_3) δ 8.20 (2H, d, $J = 7.1$ Hz), 7.65 (1H, t, $J = 7.4$ Hz), 7.52 (2H, t, $J = 7.8$ Hz), 7.15 (2H, m), 7.12 (2H, t, $J = 8.1$ Hz); ^{13}C NMR (100 MHz, CDCl_3) δ 165.1, 160.2 (d, $J = 242.7$ Hz), 146.7, 133.6, 130.1, 129.2, 128.5, 123.0 (d, $J = 8.5$ Hz), 116.1 (d, $J = 23.3$ Hz); IR (KBr) 3454, 3065, 2926, 2854, 1886, 1733, 1599, 1584, 1504, 1450, 1416, 1316, 1266, 1186, 1088, 1064, 1024, 1013 cm^{-1} ; HRMS (EI+) calcd for $\text{C}_{13}\text{H}_9\text{O}_2\text{F}$ 216.05866, found 216.05698.

Phenyl *p*-phenylbenzoate (**16**): white solid; mp 146–149 °C; 29%; ^1H NMR (400 MHz, CDCl_3) δ ; ^{13}C NMR (100 MHz, CDCl_3) δ : 8.27 (2H, d, $J = 8.4$ Hz), 7.74 (2H, d, $J = 8.4$ Hz), 7.66 (2H, d, $J = 7.2$ Hz), 7.49 (2H, m), 7.42 (2H, m), 7.29 (2H, d, $J = 7.4$ Hz), 7.24 (2H, m); ^{13}C NMR

(100 MHz, CDCl_3) δ 165.0, 151.0, 146.3, 139.8, 130.7, 129.5, 128.9, 128.3, 128.2, 127.3, 127.2, 125.8, 121.7; IR (KBr) 2919, 1730, 1456, 1404, 1264, 1196, 1083 cm^{-1} ; HRMS (EI+) calcd for $\text{C}_{19}\text{H}_{14}\text{O}_2$ 274.09938, found 274.09877.

6-Quinoliny benzoate (**17**): (synthesized from benzoyl chloride) white solid; mp 77–79 °C; 69%; ^1H NMR (400 MHz, CDCl_3) δ 8.92 (1H, d, $J = 2.92$ Hz), 8.24 (2H, d, $J = 7.12$ Hz), 8.18 (1H, d, $J = 9.12$ Hz), 8.14 (1H, dd, $J = 0.96, 8.36$ Hz), 7.70 (1H, d, $J = 2.52$ Hz), 7.66 (1H, m), 7.59 (1H, dd, $J = 2.56, 9.08$ Hz), 7.53 (2H, m), 7.42 (1H, dd, $J = 4.24, 8.32$ Hz); ^{13}C NMR (100 MHz, CDCl_3) δ 165.16, 150.26, 148.78, 146.33, 135.86, 133.87, 131.08, 130.25, 129.23, 128.69, 128.61, 124.88, 121.63, 118.62.

Phenyl 9-phenanthroate (**18**): white solid; mp 105–107 °C; 65%; ^1H NMR (400 MHz, CDCl_3) δ 9.07 (1H, m), 8.76 (3H, m), 8.04 (1H, d, $J = 7.72$ Hz), 7.80 (1H, m), 7.72 (3H, m), 7.50 (2H, m), 7.33 (3H, m); ^{13}C NMR (100 MHz, CDCl_3) δ 165.8, 151.0, 133.6, 132.5, 130.7, 130.2, 129.9, 129.5, 129.3, 129.1, 127.6, 127.1, 127.0, 126.5, 125.9, 124.9, 122.8, 122.7, 121.9; HRMS (EI+) calcd for $\text{C}_{21}\text{H}_{14}\text{O}_2$ 298.09938, found 298.09928.

O-(4-Methoxyphenyl)-*N*-methyl-*N*-phenyl thiocarbamate (**20**): procedure D; white solid; mp 109–111 °C; 91%; ^1H NMR (400 MHz, CDCl_3) δ 7.44 (2H, m), 7.33 (3H, m), 6.90 (4H, m), 3.78 (3H, s), 3.74 (3H, s); ^{13}C NMR (100 MHz, CDCl_3) δ 188.5, 157.3, 147.6, 143.5, 129.4, 127.7, 125.6, 123.2, 114.1, 55.5, 44.8; IR (KBr) 3059, 3003, 2930, 2835, 1596, 1505, 1495, 1477, 1380, 1295, 1277, 1250, 1207, 1171, 1121, 1103, 1073, 1033, 1007 cm^{-1} ; HRMS (EI+) calcd for $\text{C}_{15}\text{H}_{15}\text{O}_2\text{NS}$ 273.08235, found 273.08181.

O-(4-Cyanophenyl)-*N*-methyl-*N*-phenyl thiocarbamate (**21**): procedure D; white solid; mp 93–95 °C, 93%; ^1H NMR (400 MHz, CDCl_3) δ 7.63 (2H, d, $J = 8.5$ Hz), 7.45 (2H, t, $J = 7.4$ Hz), 7.33 (3H, m), 7.12 (2H, d, $J = 8.6$ Hz), 3.73 (3H, s); ^{13}C NMR (100 MHz, CDCl_3) δ 186.4, 157.0, 143.1, 133.3, 129.6, 128.1, 125.4, 123.9, 118.3, 109.7, 44.9; IR (KBr) 3099, 3062, 2930, 2854, 2228, 1953, 1903, 1776, 1731, 1669, 1599, 1479, 1384, 1292, 1218, 1159, 1122, 1085, 1017, 1024, 1003 cm^{-1} ; HRMS (EI+) calcd for $\text{C}_{15}\text{H}_{12}\text{ON}_2\text{S}$ 268.06704, found 268.06694.

O-(4-Methylphenyl)-*N*-methyl-*N*-phenyl thiocarbamate (**22**): procedure D; white solid; mp 75–77 °C, 90%; ^1H NMR (400 MHz, CDCl_3) δ 7.44 (2H, m), 7.33 (3H, t, $J = 6.4$ Hz), 7.15 (2H, d, $J = 7.6$ Hz), 6.94 (2H, d, 7.6 Hz), 3.74 (3H, s), 2.33 (3H, s); ^{13}C NMR (100 MHz, CDCl_3) δ 188.3, 151.8, 143.5, 135.5, 129.7, 129.4, 127.6, 125.6, 122.1, 44.7, 20.9; IR (KBr) 3061, 3034, 2923, 1884, 1749, 1595, 1506, 1500, 1477, 1448, 1379, 1291, 1276, 1217, 1180, 1121, 1089, 1073, 1018, 1003 cm^{-1} ; HRMS (ESI+) calcd for $\text{C}_{15}\text{H}_{15}\text{ONS}$ 280.07720 $[\text{M} + \text{Na}]^+$, found 280.07765 $[\text{M} + \text{Na}]^+$.

O-(3-Methylphenyl)-*N*-methyl-*N*-phenyl thiocarbamate (**23**): procedure D; white solid; mp 82–84 °C; 87%; ^1H NMR (400 MHz, CDCl_3) δ 7.44 (2H, m), 7.33 (3H, m), 7.24 (2H, m), 7.04–6.83 (3H, m), 3.75 (3H, s), 2.34 (3H, s); ^{13}C NMR (100 MHz, CDCl_3) δ 187.9, 153.9, 143.4, 139.2, 129.3, 128.7, 127.5, 126.6, 125.5, 122.9, 119.4, 44.6, 21.2; IR (KBr) 3037, 2919, 1587, 1493, 1478, 1379, 1243, 1157, 1119, 1002 cm^{-1} ; HRMS (EI+) calcd for $\text{C}_{15}\text{H}_{15}\text{ONS}$ 280.07720 $[\text{M} + \text{Na}]^+$, found 280.07971 $[\text{M} + \text{Na}]^+$.

O-(4-Chlorophenyl)-*N*-methyl-*N*-phenyl thiocarbamate (**24**): procedure D; white solid; mp 105–107 °C; 97%; ^1H NMR (400 MHz, CDCl_3) δ 7.46 (2H, t, $J = 7.4$ Hz), 7.35 (5H, m), 6.95 (2H, d, $J = 8.5$ Hz), 3.73 (3H, s); ^{13}C NMR (100 MHz, CDCl_3) δ 187.5, 152.4, 143.3, 131.3, 129.5, 129.2, 127.8, 125.5, 123.9, 44.8; IR (KBr) 3090, 3074, 3061, 2976, 2932, 2771, 2561, 2422, 2334, 2258, 2172, 2087, 2015, 1976, 1949, 1909, 1885, 1870, 1819, 1791, 1739, 1676, 1645, 1595, 1485, 1453, 1429, 1391, 1313, 1284, 1214, 1162, 1128, 1086, 1072, 1029, 1015, 1002 cm^{-1} ; HRMS (ESI+) calcd for $\text{C}_{14}\text{H}_{12}\text{ONSCl}$ 300.02258 $[\text{M} + \text{Na}]^+$, found 300.02547 $[\text{M} + \text{Na}]^+$.

O-(4-Methoxycarbonylphenyl)-*N*-methyl-*N*-phenyl thiocarbamate (**25**): procedure E; white solid; mp 108–110 °C; 71%; ^1H NMR (400 MHz,

CDCl₃) δ 8.03 (2H, d, *J* = 8.4 Hz), 7.44 (2H, m), 7.33 (3H, m), 7.07 (2H, d, *J* = 8.48 Hz), 3.89 (3H, s), 3.73 (3H, s); ¹³C NMR (100 MHz, CDCl₃) δ 186.9, 166.1, 157.3, 143.2, 130.7, 129.4, 127.7, 127.6, 125.4, 122.6, 52.0, 44.7; IR (KBr) IR (KBr) 2925, 1723, 1599, 1495, 1386, 1277, 1175, 1109, 1010 cm⁻¹; HRMS (EI+) calcd for C₁₆H₁₅O₃NS 324.06703 [M + Na]⁺, found 324.06975 [M + Na]⁺.

O-(4-Phenylphenyl)-*N*-methyl-*N*-phenyl thiocarbamate (**26**): procedure E; white solid; mp 128–130 °C; 82%; ¹H NMR (400 MHz, CDCl₃) δ 7.57 (4H, m), 7.44 (4H, m), 7.35 (4H, m), 7.10 (2H, d, *J* = 8.08 Hz), 3.77 (3H, s); ¹³C NMR (100 MHz, CDCl₃) δ 187.8, 153.3, 143.4, 140.2, 138.9, 129.3, 128.6, 127.8, 127.6, 127.2, 127.0, 125.5, 122.6, 44.7; IR (KBr) 2920, 1595, 1595, 1381, 1225, 1180, 1118, 1006 cm⁻¹; HRMS (EI+) calcd for C₂₀H₁₇ONS 342.09285 [M + Na]⁺, found 342.09564 [M + Na]⁺.

O-(1-Naphthyl)-*N*-methyl-*N*-phenyl thiocarbamate (**27**): Procedure D; white solid; mp 99–101 °C, 78%; ¹H NMR (400 MHz, CDCl₃) δ 7.85 (1H, m), 7.71 (2H, m), 7.47 (7H, m), 7.36 (1H, m), 7.19 (1H, d, *J* = 7.4), 3.81 (3H, s); ¹³C NMR (100 MHz, CDCl₃) δ 186.9, 148.9, 142.6, 133.5, 128.5, 127.0, 126.8, 126.3, 125.3, 125.2, 125.0, 124.6, 124.1, 120.4, 118.2, 43.8; IR (KBr) 3059, 2929, 1597, 1493, 1477, 1448, 1379, 1291, 1276, 1256, 1227, 1180, 1166, 1153, 1125, 1073, 1024, 1012 cm⁻¹; HRMS (ESI+) calcd for C₁₈H₁₅ONS 316.07720 [M + Na]⁺, found 316.07901 [M + Na]⁺.

O-(2-Naphthyl)-*N*-methyl-*N*-phenyl thiocarbamate (**28**): procedure D; white solid; mp 129–131 °C; 88%; ¹H NMR (400 MHz, CDCl₃) δ 7.78 (3H, m), 7.41 (5H, m), 7.31 (3H, m), 7.19 (1H, m), 3.74 (3H, s); ¹³C NMR (100 MHz, CDCl₃) δ 188.06, 151.63, 143.58, 133.68, 131.55, 129.53, 129.04, 127.90, 127.81, 127.74, 126.54, 125.79, 125.71, 122.26, 119.35; HRMS (ESI+) calcd for C₁₈H₁₅ONS 294.09526 [M + H]⁺, found 294.09548 [M + H]⁺.

O-(6-Quinolinyl)-*N*-methyl-*N*-phenyl thiocarbamate (**29**): procedure F; white solid; mp 124–126 °C; 35%; ¹H NMR (400 MHz, CDCl₃) δ 8.88 (1H, m), 8.09 (2H, m), 7.42 (7H, m), 3.77 (3H, s); ¹³C NMR (100 MHz, CDCl₃) δ 187.6, 151.7, 150.2, 146.4, 143.4, 135.8, 130.6, 129.5, 128.4, 127.9, 125.9, 125.6, 121.5, 119.2, 44.9; HRMS (ESI+) calcd for C₁₇H₁₄ON₂S 295.09051 [M + H]⁺, found 295.09110 [M + H]⁺.

O-Phenyl-*N,N*-diethyl thiocarbamate. Procedure D was followed with the only exception that Et₃N (dealkylating procedure of Millan and Prager)³⁵ has been used instead of *N*-methylaniline.

4-Methoxy-*N*-methyl-*N*-phenylbenzamide (**30**): pale yellow oil; 80%; ¹H NMR (400 MHz, CDCl₃) δ 7.25 (4H, m), 7.14 (1H, t, *J* = 7.3 Hz), 7.04 (2H, d, *J* = 7.7 Hz), 6.66 (2H, d, *J* = 8.7 Hz), 3.74 (3H, s), 3.48 (3H, s); ¹³C NMR (100 MHz, CDCl₃) δ HRMS (EI+) calcd for C₁₅H₁₅O₂N 241.11028, found 241.11020.

4-Methyl-*N*-methyl-*N*-phenylbenzamide (**31**): pale yellow oil; 72%; ¹H NMR (400 MHz, CDCl₃) δ 7.20 (4H, m), 7.13 (1H, tt, *J* = 1.2, 6.6 Hz), 7.03 (2H, d, *J* = 7.2 Hz), 6.95 (2H, d, *J* = 7.8 Hz), 3.48 (3H, s), 2.24 (3H, s); ¹³C NMR (100 MHz, CDCl₃) δ 170.7, 145.2, 139.8, 132.9, 129.1, 128.9, 128.3, 126.8, 126.3, 38.5, 21.3; IR (KBr) 2922, 1644, 1595, 1495, 1418, 1364, 1301, 1106, 1030 cm⁻¹; HRMS (EI+) calcd for C₁₅H₁₅ON 225.11537, found 225.11457.

3-Methyl-*N*-methyl-*N*-phenylbenzamide (**32**): pale yellow oil; 76%; ¹H NMR (400 MHz, CDCl₃) δ 7.24–7.18 (3H, m), 7.13 (1H, tt, *J* = 1.2, 6.6 Hz), 7.03 (H, m), 6.99 (H, m), 3.48 (3H, s), 2.21 (3H, s); ¹³C NMR (100 MHz, CDCl₃) δ 170.8, 144.9, 137.5, 135.8, 130.2, 129.4, 129.0, 127.4, 126.8, 126.3, 125.7, 38.3, 21.1; IR (KBr) 3039, 2921, 1646, 1585, 1495, 1363, 1302, 1158, 1106, 1032 cm⁻¹; HRMS (EI+) calcd for C₁₅H₁₅ON 225.11402, found 225.11475.

4-Methoxycarbonyl-*N*-methyl-*N*-phenylbenzamide (**33**): white solid; mp 78–80 °C; 97%; ¹H NMR (400 MHz, CDCl₃) δ 7.83 (2H, d, *J* = 8.4 Hz), 7.34 (2H, d, *J* = 8.4 Hz), 7.21 (2H, m), 7.14 (1H, tt, *J* = 1.2, 6.2 Hz), 7.01 (2H, d, *J* = 7.4 Hz), 3.86 (3H, s), 3.50 (3H, s); ¹³C NMR (100 MHz, CDCl₃) δ 169.6, 166.3, 144.2, 140.2, 130.7, 129.2, 129.0, 128.5,

126.9, 52.2, 38.2; IR (KBr) 2952, 1723, 1645, 1595, 1496, 1436, 1370, 1278, 1178, 1108, 1020 cm⁻¹; HRMS (EI+) calcd for C₁₆H₁₅O₃N 269.10520, found 269.10487.

4-Phenyl-*N*-methyl-*N*-phenylbenzamide (**34**): white solid; mp 99–102 °C; >99%; ¹H NMR (400 MHz, CDCl₃) δ 7.51 (2H, m), 7.36 (7H, m), 7.24 (2H, m), 7.15 (1H, m), 7.06 (2H, m), 3.52 (3H, s); ¹³C NMR (100 MHz, CDCl₃) δ 170.3, 144.9, 142.2, 140.1, 134.6, 129.3, 129.2, 128.7, 127.7, 127.0, 126.9, 126.5, 126.3, 38.5; IR (KBr) 3031, 2923, 1644, 1595, 1495, 1419, 1364, 1301, 1281, 1106, 1008 cm⁻¹; HRMS (EI+) calcd for C₂₀H₁₇ON 287.13102, found 287.13032.

N-Methyl-*N*-phenyl-2-naphthamide (**35**): white solid, mp 84 °C; 79%; ¹H NMR (400 MHz, CDCl₃) δ 7.89 (1H, s), 7.71 (2H, m), 7.58 (1H, d, *J* = 8.56), 7.45 (2H, pd, *J* = 1.4, 6.84 Hz), 7.31 (1H, dd, *J* = 1.64, 8.56 Hz), 7.19 (2H, m), 7.09 (3H, m); ¹³C NMR (100 MHz, CDCl₃) δ 187.66, 151.70, 150.25, 146.40, 143.45, 135.84, 130.61, 129.57, 128.43, 127.93, 125.93, 125.64, 121.52, 119.24, 44.90; HRMS (CI+) calcd for C₁₈H₁₆ON 262.12319, found 262.12351.

■ ASSOCIATED CONTENT

Supporting Information. ¹H and ¹³C NMR spectra. Total energy and Cartesian coordinates for each optimized stationary point at the reaction hyper surfaces. This material is available free of charge via the Internet at <http://pubs.acs.org>.

■ AUTHOR INFORMATION

Corresponding Author

*E-mail: alabugin@chem.fsu.edu.

■ ACKNOWLEDGMENT

I.A. is grateful to the National Science Foundation (CHE-0848686) for partial support of this research. We are grateful to the high-performance computing facility at FSU for providing computational resources for the DFT calculations.

■ REFERENCES

- (1) Barnard, C. F. J. *Organometallics* **2008**, *27*, 5402. Brennfuhrer, A.; Neumann, H.; Beller, M. *Angew. Chem., Int. Ed.* **2009**, *48*, 4114. Lou, R.; VanAlstine, M.; Sun, X.; Wentland, M. P. *Tetrahedron Lett.* **2003**, *44*, 2477. Rahman, O.; Kihlberg, T.; Långström, B. *J. Org. Chem.* **2003**, *68*, 3558. Rahman, O.; Kihlberg, T.; Långström, B. *J. Chem. Soc. Perkin Trans. 1* **2002**, 2699. Gerlach, U.; Wollmann, T. *Tetrahedron Lett.* **1992**, *33*, 5499. Cacchi, S.; Lupi, A. *Tetrahedron Lett.* **1992**, *33*, 3939. Dolle, R. E.; Schmidt, S. J.; Kruse, L. I. *J. Chem. Soc. Chem. Commun.* **1987**, 904. Cacchi, S.; Ciattini, P. G.; Morera, E.; Ortari, G. *Tetrahedron Lett.* **1986**, *27*, 3931.
- (2) Committee for Human Medicinal Products (CHMP). CPMP/SWP/QWP/4446/2000 Guideline on the Specification Limits for Residues of Metal Catalysts or Metal Reagents. http://www.ema.europa.eu/docs/en_GB/document_library/Scientific_guideline/2009/09/WC500003586.pdf. accessed Feb 15, 2011.
- (3) Langley, D. R.; Golik, J.; Krishnan, B.; Doyle, T. W.; Beveridge, D. L. *J. Am. Chem. Soc.* **1994**, *116*, 15.
- (4) (a) Jones, R. R.; Bergman, R. G. *J. Am. Chem. Soc.* **1972**, *94*, 660. (b) Bergman, R. G. *Acc. Chem. Res.* **1973**, *6*, 25.
- (5) (a) Baroudi, A.; Mauldin, J.; Alabugin, I. V. *J. Am. Chem. Soc.* **2010**, *132*, 967. For our preliminary work on the multiple roles of ortho-substituents in the Bergman cyclization, see: (b) Zeidan, T. A.; Manoharan, M.; Alabugin, I. V. *J. Org. Chem.* **2006**, *71*, 954. (c) Zeidan, T.; Kovalenko, S. V.; Manoharan, M.; Alabugin, I. V. *J. Org. Chem.* **2006**, *71*, 962. (d) Pickard, F. C.; Shepherd, R. L.; Gillis, A. E.; Dunn, M. E.; Feldgus, S.; Kirschner, K. N.; Shields, G. C.; Manoharan, M.; Alabugin,

I. V. J. *Phys. Chem. A* **2006**, *110*, 2517. (e) Alabugin, I. V.; Manoharan, M. *J. Phys. Chem. A* **2003**, *107*, 3363. (f) Alabugin, I. V.; Manoharan, M.; Kovalenko, S. V. *Org. Lett.* **2002**, *4*, 1119.

(6) Falvey, D. E.; Khambatta, B. S.; Schuster, G. B. *J. Phys. Chem.* **1990**, *94*, 1056.

(7) For another example of the use of oxygen in the C–C bond formation at the ipso-position, see: Vasilevsky, S. F.; Baranov, D. S.; Mamatyuk, V. I.; Gatilov, Y. V.; Alabugin, I. V. *J. Org. Chem.* **2009**, *74*, 6143.

(8) A similar approach, which occurs through a five-membered transition state (1,4 O→C transposition), was used in the total synthesis of the aromatic series of podophyllotoxin: Reynold, A. J.; Scott, A. J.; Turner, C. I.; Sherburn, M. S. *Am. Chem. Soc.* **2003**, *125*, 12108. Fischer, J.; Reynold, A. J.; Sharp, L. A.; Sherburn, M. S. *Org. Lett.* **2004**, *6*, 1345.

(9) (a) Banks, J. T.; Scaiano, J. C. *J. Phys. Chem.* **1995**, *99*, 3527. (b) Donkers, R. L.; Tse, J.; Workentin, M. S. *Chem. Commun.* **1999**, 135. (c) Wietzerbin, K.; Bernadou, J.; Meunier, B. *Eur. J. Inorg. Chem.* **1999**, 1467. (d) Kamata, M.; Komatsu, K. *Tetrahedron Lett.* **2001**, *42*, 9027. (e) Studer, A.; Bossart, M. *Tetrahedron* **2001**, *57*, 9649. (f) Donkers, R. L.; Workentin, M. S. *J. Am. Chem. Soc.* **2004**, *126*, 1688. (g) Antunes, C. S. A.; Bietti, M.; Ercolani, G.; Lanzalunga, O.; Salamone, M. *J. Org. Chem.* **2005**, *70*, 3884. (h) Bietti, M.; Salamone, M. *J. Org. Chem.* **2005**, *70*, 10603. (i) Ingold, K. U.; Smeu, M.; DiLabio, G. A. *J. Org. Chem.* **2006**, *71*, 9906.

(10) In contrast, anionic 1,2 O→C transpositions proceed often from a C-centered anion to an O-centered anion: Wittig, G.; Lohmann, L. *Liebigs Ann.* **1942**, *550*, 260. Reviews: Marshall, J. A. The Wittig rearrangement. In *Comprehensive Organic Synthesis*; Trost, B. M., Fleming, I., Eds.; Pergamon: Oxford, 1991; Vol. 3, pp 975–1014. Tomooka, K.; Yamamoto, H.; Nakai, T. *Liebigs Ann.* **1997**, 1275. An interesting recent example of a pyridine ring migration: Yang, J.; Dudley, G. B. *J. Org. Chem.* **2009**, *74*, 7998. However, transformations of alkoxides to carbanions through 1,2-shifts are also known: Brook, A. G. *J. Am. Chem. Soc.* **1958**, *80*, 1886. Brook, A. G. *Acc. Chem. Res.* **1974**, *7*, 77. Jankowski, P.; Raubo, P.; Wicha, J. *Synlett* **1994**, 985.

(11) (a) Baroudi, A.; Alicea, J.; Alabugin, I. V. *Chem.—Eur. J.* **2010**, *16*, 7683. (b) Baroudi, A.; Flack, P.; Alabugin, I. V. *Chem.—Eur. J.* **2010**, *16*, 12316.

(12) Ohno, A.; Kito, N.; Ohnishi, Y. *Bull. Chem. Soc. Jpn.* **1971**, *44*, 467.

(13) Sarma, S. J.; Jones, P. B. *J. Org. Chem.* **2010**, *75*, 3806.

(14) (a) Barton, D. H. R.; McCombie, S. W. *J. Chem. Soc., Perkin Trans. 1* **1975**, 1574. (b) Barton, D. H. R.; Crich, D.; Löbberding, A.; Zard, S. Z. *J. Chem. Soc., Chem. Commun.* **1985**, 646. (c) Barton, D. H. R.; Crich, D.; Löbberding, A.; Zard, S. Z. *Tetrahedron* **1986**, *42*, 2329. (d) Barton, D. H. R. *Half a Century of Free Radical Chemistry*; Cambridge University Press: Cambridge, 1993. (e) Zard, S. Z. *Aust. J. Chem.* **2006**, *59*, 663.

(15) Tris(trimethylsilyl)silane (TTMSS, Chatgililoglu, C. *Chem.—Eur. J.* **2008**, *14*, 2310) was also found to be a possible source of Si-centered radicals. However, in our hands, the rearrangement with this silane suffered from poor reproducibility. This problem can be partially rectified by the use of polarity reversal catalysis by thiols (vide infra).

(16) (a) Zimmerman, H. E.; Rieke, R. D.; Scheffer, J. R. *J. Am. Chem. Soc.* **1967**, *89*, 2033–2047. (a) Zimmerman, H. E.; Alabugin, I. V.; Chen, W.; Zhu, Z. *J. Am. Chem. Soc.* **1999**, *121*, 11930–11931.

(17) (a) Nunez, A.; Sánchez, A.; Burgos, C.; Alvarez-Builla, J. *Tetrahedron* **2004**, *60*, 6217. (b) Harrowven, D. C.; Woodcock, T.; Howes, P. D. *Angew. Chem., Int. Ed.* **2005**, *44*, 3899. (c) Curran, D. P.; Keller, A. I. *J. Am. Chem. Soc.* **2006**, *128*, 13706.

(18) Schleyer, P. v. R.; Puhlhofer, F. *Org. Lett.* **2002**, *4*, 2873. See also: Stahl, F.; Moran, D.; Schleyer, P. v. R.; Prall, M.; Schreiner, P. R. *J. Org. Chem.* **2002**, *67*, 1453. Alabugin, I. V.; Manoharan, M.; Breiner, B.; Lewis, F. J. *Am. Chem. Soc.* **2003**, *125*, 9329–9342.

(19) The relatively high reactivity of the polycyclic compound leads to the formation of other minor unidentified byproduct leading to the lower reaction yields.

(20) Dewar, M. J. S.; Dougherty, R. C. *The PMO Theory of Organic Chemistry*; Plenum Press: New York, 1976; pp 117–140.

(21) (a) Escoubet, S.; Gastaldi, S.; Vanthuyne, N.; Gil, G.; Siri, D.; Bertrand, M. P. *Eur. J. Org. Chem.* **2006**, 3242. (b) Escoubet, S.; Gastaldi, S.; Vanthuyne, N.; Gil, G.; Siri, D.; Bertrand, M. P. *J. Org. Chem.* **2006**, *71*, 7288.

(22) (a) Bietti, M.; Ercolani, G.; Salamone, M. *J. Org. Chem.* **2007**, *72*, 4515. (b) Smeu, M.; DiLabio, G. A. *J. Org. Chem.* **2007**, *72*, 4520.

(23) The C–O bond fragmentation barrier for this radical is 11 kcal/mol as it is exothermic by 14 kcal/mol at the UB3LYP/6-31+G** level.

(24) (a) For a detailed analysis of factors controlling donor ability of nitrogen lone pairs, see: Alabugin, I. V.; Manoharan, M.; Zeidan, T. A. *J. Am. Chem. Soc.* **2003**, *125*, 14014. (b) See also: Alabugin, I. V.; Manoharan, M. *J. Comput. Chem.* **2007**, *28*, 373–390. Alabugin, I. V.; Manoharan, M.; Buck, M.; Clark, R. J. *THEOCHEM* **2007**, *813*, 21.

(25) Extensive work on modifying reaction conditions for the TTMSS-promoted reactions did not lead to their reproducibility. In fact, careful purification of carbonates, silane, and radical initiators seemed to have no effect on reaction yields. Only in the presence of thiol additives, formation of the rearranged products was reproducible when TTMSS was used.

(26) Our calculations at the UB3LYP/6-31+G** level suggest that H-transfer from Et₃SiH to Et₃SiS radical is exothermic by 6 kcal/mol. For further information about similar reactions and polarity reversal catalysis, see: (a) Cole, S. J.; Kirwan, J. N.; Roberts, B. P.; Willis, C. R. *J. Chem. Soc., Perkin Trans. 1* **1991**, 103. (b) Roberts, B. P. *Chem. Soc. Rev.* **1999**, *28*, 25. (c) Cai, Y.; Roberts, B. P. *J. Chem. Soc., Perkin Trans. 2* **2002**, 1858. (d) Chatgililoglu, C. *Organosilanes in Radical Chemistry*; Wiley: New York, 2004. (e) Schiesser, C. H.; Skidmore, M. A. *J. Chem. Soc., Perkin Trans. 2: Phys. Org. Chem.* **1998**, 2329–2332. (f) Guin, J.; Mueck-Lichtenfeld, C.; Grimme, S.; Studer, A. *J. Am. Chem. Soc.* **2007**, *129*, 4498–4503. (g) Crich, D.; Grant, D.; Krishnamurthy, V.; Patel, M. *Acc. Chem. Res.* **2007**, *40*, 453.

(27) (a) Studer, A. In *Radicals in Organic Synthesis*; Renaud, P., Sibi, M. P., Eds.; Wiley-VCH: Weinheim, 2001; Vol. 2, pp 44–60. (b) Studer, A.; Bossart, M. *Tetrahedron* **2001**, *57*, 9649.

(28) Bacqué, E.; El Qacemi, M.; Zard, Z. S. *Org. Lett.* **2005**, *7*, 3817.

(29) The differences may be associated with the lower stabilization of the reactant C-radical and greater stabilization of N-radical product in comparison to our cascades. Also note that the product composition is very sensitive to substitution and the reaction conditions; high yields of the transposed product were only observed for the t-Bu-substituted amines.

(30) Frisch, M. J.; Trucks, G. W.; Schlegel, H. B.; Scuseria, G. E.; Robb, M. A.; Cheeseman, J. R.; Montgomery, J. A., Jr.; Vreven, T.; Kudin, K. N.; Burant, J. C.; Millam, J. M.; Iyengar, S. S.; Tomasi, J.; Barone, V.; Mennucci, B.; Cossi, M.; Scalmani, G.; Rega, N.; Petersson, G. A.; Nakatsuji, H.; Hada, M.; Ehara, M.; Toyota, K.; Fukuda, R.; Hasegawa, J.; Ishida, M.; Nakajima, T.; Honda, Y.; Kitao, O.; Nakai, H.; Klene, M.; Li, X.; Knox, J. E.; Hratchian, H. P.; Cross, J. B.; Adamo, C.; Jaramillo, J.; Gomperts, R.; Stratmann, R. E.; Yazyev, O.; Austin, A. J.; Cammi, R.; Pomelli, C.; Ochterski, J. W.; Ayala, P. Y.; Morokuma, K.; Voth, G. A.; Salvador, P.; Dannenberg, J. J.; Zakrzewski, V. G.; Dapprich, S.; Daniels, A. D.; Strain, M. C.; Farkas, O.; Malick, D. K.; Rabuck, A. D.; Raghavachari, K.; Foresman, J. B.; Ortiz, J. V.; Cui, Q.; Baboul, A. G.; Clifford, S.; Cioslowski, J.; Stefanov, B. B.; Liu, G.; Liashenko, A.; Piskorz, P.; Komaromi, I.; Martin, R. L.; Fox, D. J.; Keith, T.; Al-Laham, M. A.; Peng, C. Y.; Nanayakkara, A.; Challacombe, M.; Gill, P. M. W.; Johnson, B.; Chen, W.; Wong, M. W.; Gonzalez, C.; Pople, J. A. *Gaussian 03, Revision C.02*; Gaussian: Wallingford, CT, 2004.

(31) This method has been successfully used to describe a number of radical reactions: (a) Fischer, H.; Radom, L. *Angew. Chem., Int. Ed.* **2001**, *40*, 1340 and references cited therein. (b) Schreiner, P. R.; Navarro-Vazquez, A.; Prall, M. *Acc. Chem. Res.* **2005**, *38*, 29 and references cited therein. (c) Hrovat, D. A.; Beno, B. R.; Lange, H.; Yoo, H. Y.; Houk, K. N.; Borden, W. T. *J. Am. Chem. Soc.* **1999**, *121*, 10529. (d) Saettel, N. J.; Wiest, O.; Singleton, D. A.; Meyer, M. P. *J. Am. Chem. Soc.* **2002**, *124*, 11552. (e) Alabugin, I. V.; Manoharan, M. *J. Am. Chem. Soc.* **2005**, *127*, 12583. (f) Alabugin, I. V.; Timokhin, V. I.; Abrams, J. N.; Manoharan, M.; Abrams, R.; Ghiviriga, I. *J. Am. Chem. Soc.* **2008**,

130, 10984. (g) Alabugin, I. V.; Gilmore, K.; Patil, S.; Manoharan, M.; Kovalenko, S. V.; Clark, R. J.; Ghiviriga, I. *J. Am. Chem. Soc.* **2008**, *130*, 11535.

(32) The NBO 4.0 Program: Glendening, E. D.; Badenhoop, J. K.; Reed, A. E.; Carpenter, J. E.; Weinhold, F. Theoretical Chemistry Institute, University of Wisconsin, Madison, WI, 1996.

(33) Natural bond orbital (NBO) analysis finds significant radical-stabilizing interactions via the second-order perturbation approximation as (two sets of $n(\text{O}) \rightarrow n(\text{C})$ interactions (5.1 + 22.9) + (3.4 + 28.0) and one set of $n(\text{S}) \rightarrow n(\text{C})$ (1.6 + 24.7) interactions for thiocarbonates; $n(\text{O}) \rightarrow n(\text{C})$ (3.5 + 19.0), $n(\text{N}) \rightarrow n(\text{C})$ (28.4) and $n(\text{S}) \rightarrow n(\text{C})$ (1.8 + 22.7) interactions for thiocarbamates). The energies are given in kcal/mol for the parent Ph-substituted compounds at B3LYP/6-31G(d,p) level. Two interactions given for oxygen and sulfur correspond to the two lone pairs present at these atoms (sp^n -hybrid and p-orbital). For a comparison of the donor properties of these lone pairs, see: Alabugin, I. V. *J. Org. Chem.* **2000**, *65*, 3910; Alabugin, I. V.; Gilmore, K.; Peterson, P. Hyperconjugation. *WIREs Comput. Mol. Sci.* **2011**, *1*, 109–141 DOI: 10.1002/wcms.6, and ref 24a.

(34) Salamone, M.; Bietti, M.; Calcagni, A.; Gente, G. *Org. Lett.* **2009**, *11*, 2453. Bietti, M.; Calcagni, A.; Cicero, D. O.; Martella, R.; Salamone, M. *Tetrahedron Lett.* **2010**, *51*, 4129.

(35) Millan, D. S.; Prager, R. H. *Aust. J. Chem.* **1999**, *52*, 841.